Uranium Core Design for Versatile Test Reactor

J. Harris[1], S. Henzab[2], A. Isom[1], J. Page[1], and A. Taylor[1]

[1]North Carolina State University
[2]South Carolina State University

August 12, 2025

Abstract

Today, the concept of VTR is a sodium-cooled fast reactor which provides a fast neutron spectrum environment to test advanced nuclear materials and fuels. With advanced nuclear energy fuels and designs being pursued in the United States, adequate infrastructure for experimentation, testing, design evolution, and component qualification is required. In particular, the Versatile Test Reactor's mission is to expand the United States' limited testing capabilities. Unlike the PRISM or Natrium reactors, which are designed to function as demonstration reactors, the Versatile Test Reactor (VTR) is to be a materials test reactor. Its purpose is to develop an understanding of the behavior of materials under a fast neutron flux; for this reason, it is designed to optimize fast neutron production.With the highest fast neutron flux of any reactor, it will enable hastened testing of components for new reactors, such as advanced fuel types, new cladding materials and other experiments that will further the field of nuclear engineering. [17]

In its current form, the VTR is designed to be operated using plutonium fuel, however, this type of fuel may be difficult to obtain in the future because of the lack of reactor grade plutonium the United States has stored. This, coupled with other projects such as the Plutonium Pit Production facility at Savannah River National Laboratory and NASA's planned deep space missions, puts a strain on the plutonium supply chain. This complication has led Idaho National Laboratory to consider adapting the current design for the VTR so that it may utilize high-assay low-enriched uranium (HALEU) fuel instead. Our project therefore is to design a core for the VTR which can operate using HALEU fuel while still achieving the intended fast flux of $4 \times 10^{15}\,\mathrm{cm}^{-2}\mathrm{s}^{-1}$. The challenge stems from maintaining the size of the reactor specified by INL that was designed to be operated using plutonium fuel, which has a higher fuel density than uranium, allowing it to attain a higher flux in a smaller reactor. To try to alleviate this issue, experimentation into several different types of fuels, such as uranium carbide, uranium nitride and uranium zirconium, was required.

Contents

1 What is the Versatile Test Reactor?

1.1 Introduction

With advanced nuclear energy fuels and designs being pursued in the United States, adequate infrastructure for experimentation, testing, design evolution, and component qualification is required. In particular, the Versatile Test Reactor's mission is the continued development and maturation of fast reactor technology. Unlike the PRISM or Natrium reactors, which are designed to function as demonstration reactors, the Versatile Test Reactor (VTR) is simply a test reactor. This means that its purpose is to develop an understanding of the behavior of materials under a fast neutron flux; and therefore, it is meant to optimize fast neutron production.

1.2 Alternative Research Reactors

Prior to the Versatile Test Reactor's conception, there were three reactors that portrayed the significant aspects of this project. They are:

- Experimental Breeder Reactor 2 (EBR-II)
- Fast Flux Test Facility (FFTF)
- Advanced Test Reactor (ATR)

Like the VTR, the Advanced Test Reactor functioned as a way to complete materials testing and verify applicability of certain nuclear fuels. This reactor could provide a fast flux of $4 \times 10^{14}\,\mathrm{cm}^{-2}\mathrm{s}^{-1}$. However, it lacked the fundamental quality of operating on a coolant that would be utilized in future reactors: namely sodium. The Experimental Breeder Reactor II and the Fast Flux Test Facility make up for the lack of capability to assess coolant interactions with materials: as they are both sodium cooled fast reactors as opposed to pressurized water reactors. With regards to EBR-II, the emphasis was placed on the demonstration of the breeder reactor concept using solid metallic fuel. While materials testing later became an application, it was not something which the reactor was designed to excel at. The Fast Flux Test Facility is almost identical in functionality to the Versatile Test Reactor. It operated with a peak neutron flux of $7 \times 10^{15}\,\mathrm{cm}^{-2}\mathrm{s}^{-1}$. It's main goal was the testing of nuclear fuels, components, and materials for applicability in a sodium cooled fast reactor; however, it lacked the versatility of the VTR by only operating under a single type of coolant. Unlike the reactors mentioned here, the Versatile Test Reactor is meant to simulate multiple coolant types in addition to providing a peak-fast flux and displacement per atom (for testing nuclear materials.

1.3 Design

The Versatile Test Reactor is a sodium-cooled reactor meant to operate at coolant temperatures up to 1100 °F as a result of the thermal properties of sodium.

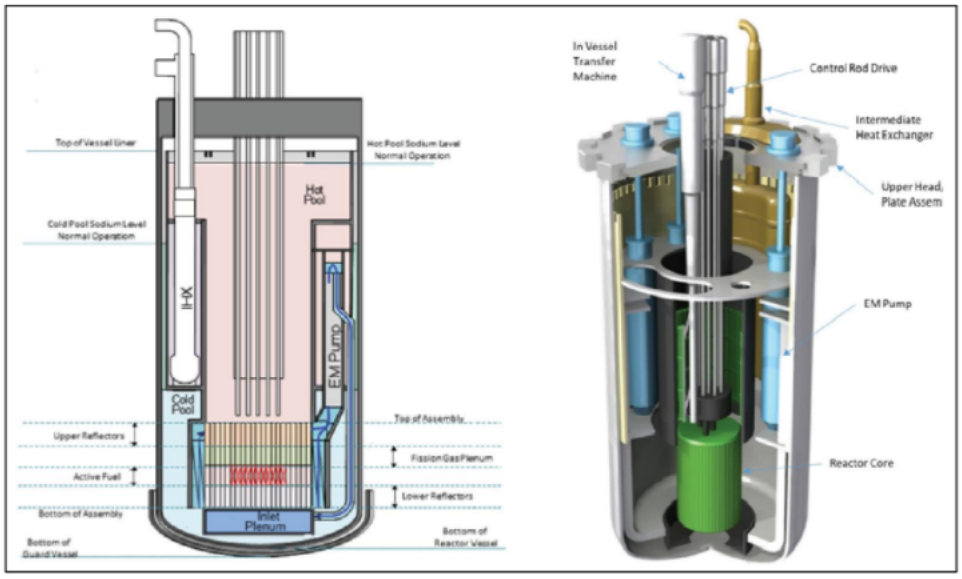

Figure 1.1: VTR Core Cross-Section

With regards to previous designs, the Versatile Test Reactor is meant to function as an improvement through the providing of a fast neutron flux of approximately $4 \times 10^{15}\,\mathrm{cm}^{-2}\mathrm{s}^{-1}$ [14]. It is also meant to have a displacement per atom (dpa) level in excess of 30 dpa/year alongside test volumes in excess of 7 L per test location; and the effective testing height is at a minimum of 60 cm. It will also have a large number of testing locations and an ability to test fuel and materials in prototypical environments other than sodium. These environments include lead, lead-bismuth, and helium. Of relevance is the design of the core itself. It has been established that the VTR core will consist of three regions: the fuel, reflector assemblies, and shield assemblies. Within the fuel region in particular, multiple testing, control, and safety assemblies are available. A graphic is provided Figure 1.2 gives a proper understanding of the types of assembly available within the core.

Driver (fuel) assembly located in the active region of the core contains the fuel needed to power the reactor and produces the fast neutron flux necessary for irradiation of test assemblies or specimens.

Reflector assembly surrounds the active central region of the core that contains driver assemblies and test assemblies and contains material to reflect neutrons back into the central part of the core.

Shield assembly is positioned outside of the reflector assemblies within the core and contains material to absorb neutrons that pass through the reflector to reduce neutron damage to the reactor structural components.

Test assembly contains the test specimen and any equipment needed to support the experiment. Instrumented test assemblies could be as long as 65 feet and are located in the active region of the core. Non-instrumented assemblies would be the same length as driver assemblies (less than 13 feet) and may be located in either the active region of the core or in the first row of reflector assemblies.

Test specimen is the material being exposed to a fast neutron flux to determine the effects of the exposure and includes any capsule necessary to support the test. The test specimen can be no more than about 31 inches long.

Control assembly provides the core startup control, power control, burnup compensation, and absorber run-in in response to demands from the plant control system. In conjunction with safety assemblies, provide a rapid shutdown capability.

Safety assembly provides redundant rapid shutdown capability.

Figure 1.2: Listing of Assembly Definitions

The design for the VTR core includes 66 assemblies of driver fuel with 271 pins available per assembly. According to the recently released Environmental Impact Statement, the core will also include 6 fixed instrumented test locations along with multiple options for non-instrumented locations in the core and reflector. The combined number of control and safety assemblies has also been designated: with 6 control and 3 safety assemblies. In addition, there are to be 114 radial reflectors and 114 radial shield reflectors within the core. The non-instrumented test locations can be positioned anywhere in the core. Figure 1.3 is a graphic from the Environmental Impact Statement is provided to display one of the expected core layouts.

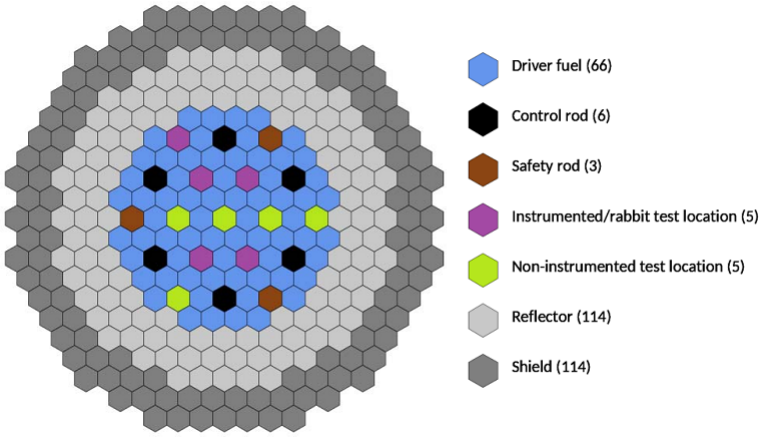

Figure 1.3: VTR Core Axial View

The total length of each assembly from the inlet nozzle end to the outlet nozzle end is approximately 3.8 m. The various areas currently modeled for each type of assembly are schematically shown in Figure 1.4.

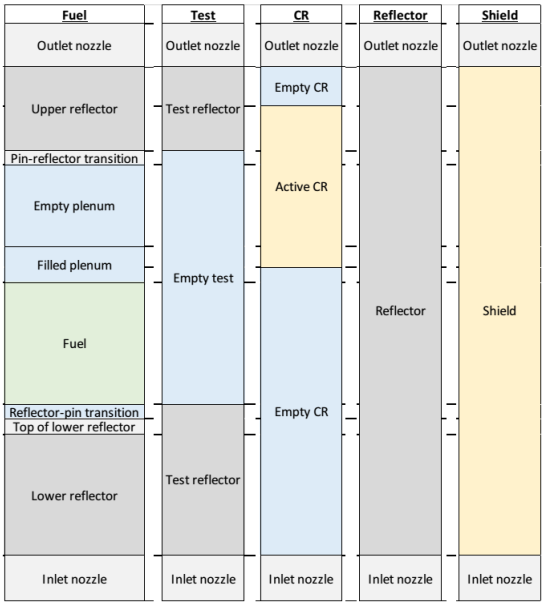

Figure 1.4: Cross Section of Each Assembly Type

At the current stage of design, geometric details have been determined only for the fuel and control rod (CR) assembly. This is because these assemblies are the most influential assemblies when it comes to core performance.

1.4 Driver Fuel Assemblies

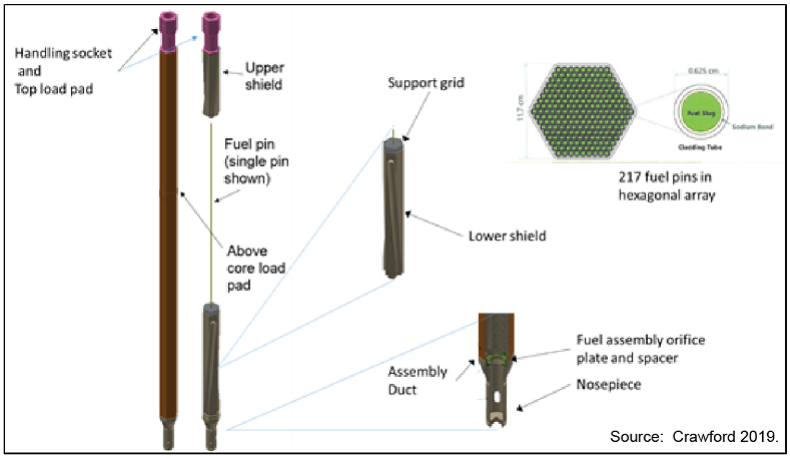

Figure 1.5: Driver Fuel Assembly

The current core design requires the usage of uranium-plutonium-zirconium fuel pins within hexagonal assemblies containing HT-9 stainless steel cladding. From the bottom to the top, the driver fuel assembly is composed of the nose-piece/inlet nozzle module, the lower shield, the fuel pin bundle, the upper shield, and the upper handling socket module; and an assembly duct stretches from the inlet to outlet modules. Overall, the driver fuel assembly is about 3.85 m meters long and it measures 11.7 cm from one flat side to the opposite flat side.

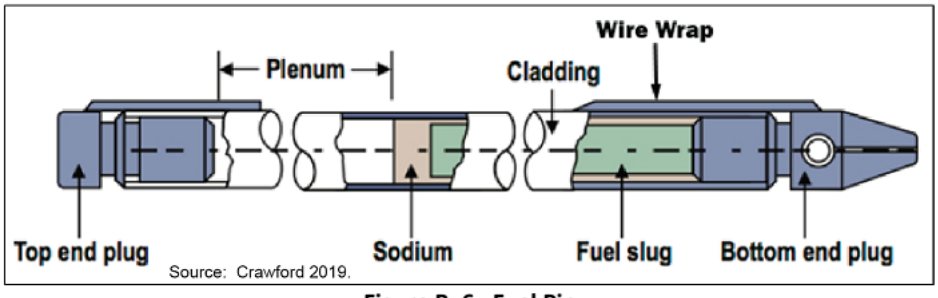

Figure 1.6: Fuel Pin Anatomy

1.5 Reflector Assemblies

The reflector assembly improves neutron efficiency by reflecting some leaked neutrons back into the core (the more neutrons produced during fission remain in the core longer). The volume inside the reflector assembly duct consists of HT-9 stainless steel rods. These rods will be tightly packed to achieve a high steel volume; and there will not be wire wraps around the rods. The HT-9 and coolant volume ratios within the reflector assembly are 0.80 and 0.20.

1.6 Shield Assemblies

Shielding assemblies protect surrounding structures (such as reactor vessels and protective vessels) from the effects of neutron radiation. The two sets of assemblies are made of a hexagonal HT-9 stainless steel duct.

1.7 Control and Safety Assemblies

The control assemblies control the changes in the reactivity and also adjust for the power level of the VTR core. The safety assemblies, which are designed in a similar fashion, are not present in the core during normal operation. Each of the control and safety assemblies are connected to a control drive mechanism located at the top of the reactor top head through a penetration in the reactor top assembly rotating plug. All nine assemblies are configured to form a dual channel assembly, with the inner channel containing a set of 37 wired shock absorber pins. The pins are made of a HT-9 stainless steel sheath and boron carbide (B4C) granules.

1.8 Test Assemblies

Test assemblies within the reactor are divided into non-instrumented and instrumented experiments. Non-instrumented experiments (i.e., specimens) can be placed at multiple locations in the reactor core or reflector area by replacing nuclear fuel or reflector assemblies. Instrumentation experiments, which can provide real-time information while the reactor is operating, require penetration of the reactor cover for the instrumentation and can only be deployed in six fixed positions.

The six instrumented test positions are provided by six penetrations for the instrumentation stalk and are connected directly through the reactor vessel head to a monitor in the experimental support area that is delivered to a rotatable

plug similar to the penetrations to the control assembly. In addition to these test assemblies, test pins may be located within the driver fuel assembly.

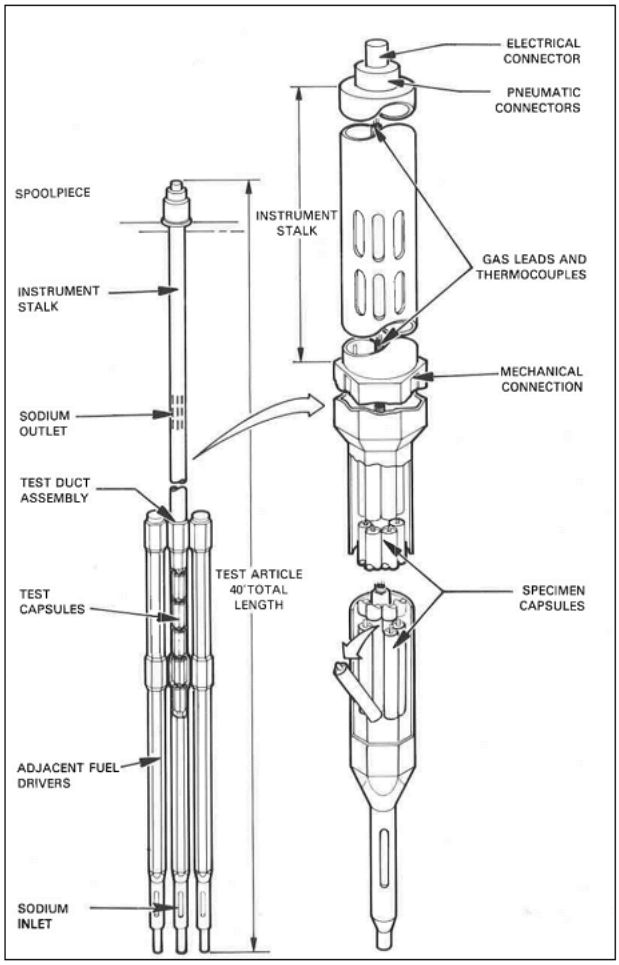

Figure B–7. Representative Instrumented Test Assembly

Figure 1.7: Instrumented Test Assembly

Based on previous experience, instrumented test assemblies include many, including those that measure local temperature, flow rate, pressure (including pressure in the fuel pin fission gas plenum), and neutron flux. The three test assembly types currently envisioned for use in the VTR are:

- Normal Test Assembly (NTA)

  - The NTAs would be the standard non-instrumented or passively instrumented open test assemblies that would be the same size, flat-to-flat, as the driver fuel assemblies; and they would use the same path and equipment as driver fuel for insertion and removal from the reactor. The experiments revolving around these assemblies would be fuels or materials.

- Extended Length Test Assembly (ELTA)
  - All ELTAs would extend through the reactor head, and typically would have various instrumentation leads that run to the Radiation and/or Non-Radiation Experiment Rooms adjacent to the Head Access Area. The ELTAs would have specialized casks capable of preheating using downward flowing argon; providing power, as necessary, to the ELTA (e.g., for cartridge loops); and the required lifting fixtures.
  - ELTAs would include fuels (ELTA-F) or materials (ELTA-M) or can be cartridge loops (ELTA CL) that could contain coolants separate from the basic sodium. Figure 3–1 provides a representative design of an ELTA-M.
  - The rabbit thimble that would go into the basic coolant would be handled by the same pathway as the ELTAs, although the rabbit thimble is not considered to be an ELTA, but would use the same infrastructure for insertion and removal.

- Rabbit Test Assembly (RTA)
  - The RTA would use a capsule that contains the experimental specimens, which would be propelled down the rabbit tube into the rabbit thimble, irradiated, and recovered during or between test cycles.
  - The RTA capsule would be very specialized with tight tolerances to ensure compatibility with the rabbit thimble, fins for heat rejection if needed, and would be qualified as an experiment containment boundary.
  - An important function of the VTR is the ability to irradiate the cartridge closed loop with VTR basic sodium and various closed loop coolants such as molten lead, molten salt, helium or sodium under different conditions. Therefore, VTR can directly support the development of lead and lead bismuth eutectic cooled fast reactors, molten salt reactors, fluoride hot reactors, hot gas cooled reactors and advanced sodium cooled fast reactor designs.

An important function of the VTR is the ability to irradiate the cartridge closed loop with VTR basic sodium and various closed loop coolants such as molten

lead, molten salt, helium or sodium under different conditions. Therefore, VTR can directly support the development of lead and lead bismuth eutectic cooled fast reactors, molten salt reactors, fluoride hot reactors, hot gas cooled reactors and advanced sodium cooled fast reactor designs.

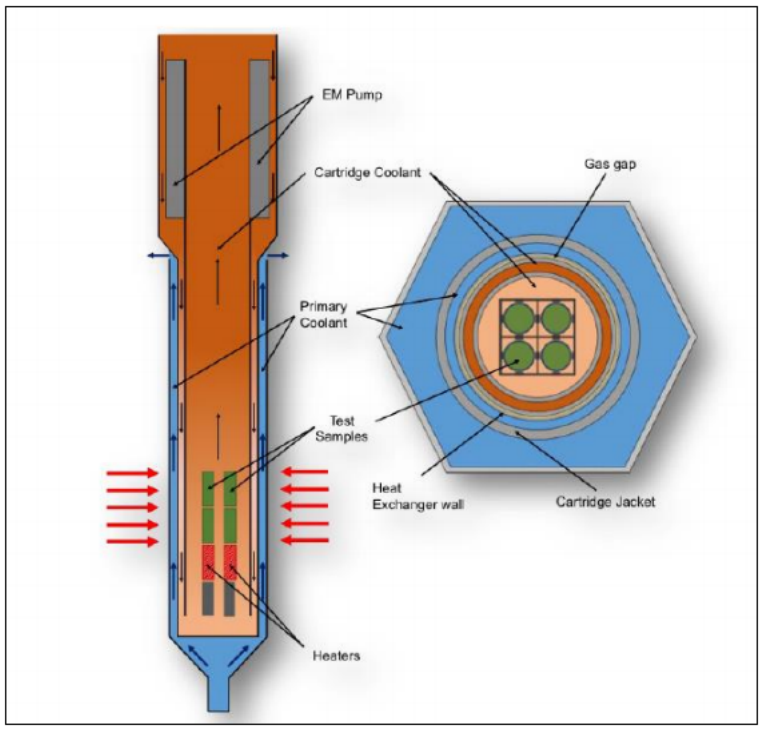

Figure B–8. Closed-Loop Cartridge Test Assembly

Figure 1.8: Closed-Loop Cartridge Test Assembly

In the VTR, closed-loop cartridge coolant flows upwards through the closed-loop fuel area and downwards through the surrounding down corners. Here, heat is rejected as sodium basic: which flows upward through a double-wall pressure boundary.

The cartridge closed loop can be similar in height to the driver fuel assembly and includes instrument leads (including instrument leads to monitor coolant purity), gas lines (some have changed coolant chemistry to eliminate corrosion of cladding and structures), and power cables.

The remaining test locations within the core and reflector are used for un-instrumented test assemblies. A non-instrumented test vehicle is a fuel assembly used to test alternative fuel concepts, cladding and structural materials that may

differ from the fuel assembly. These test assemblies maintain the same external dimensions as all fuel assemblies.

2 Problem Statement

In its current form, the Versatile Test Reactor is to operate through the use of a metallic fuel alloy of uranium, plutonium, and zirconium (U-20Pu-10Zr) with approximately 1800 kg of heavy-metal fuel required annually: with 1400 kg of uranium and 400 kg of plutonium. In place of this fuel, which could be difficult to obtain in the future, the objective is to utilize something known as High-Assay Low-Enriched Uranium (HALEU) fuel. With this, the specific feature of the VTR which must be maintained is the fast neutron flux of $4 \times 10^{15}\,\mathrm{cm}^{-2}\mathrm{s}^{-1}$.

HALEU fuel differs from the types of fuels typically utilized due to its enrichment value. The usual value of enrichment for a nuclear reactor is found to be between 0.711% and 5%. This is known as LEU. The purpose of increasing the enrichment by up to a percentage of 20, the upper limit of HALEU, is that the additional fissile material leads to higher burnup values and decreases the required size of a reactor core. Within the range for this categorization of fuel, an acceptably self-sustaining reactor core is speculated to be possible.

The types of fuel available for usage in this core design are as follows:

- Uranium Nitride (UN)
- Uranium Carbide (UC)
- Uranium Zirconium (U-10Zr)
- Uranium Oxide (UO_2)

Each of these fuel types has been tested to a certain extent due to their viability as a industrial scale nuclear fuel. With each, there is a certain depth of knowledge and cost of fabrication that must be taken into account during implementation. These were the fundamental project parameters.

2.1 Fuel Data

When observing nuclear fuels, there are certain aspects worth considering. This can vary by study, but K. L. Murty & I. Charit [16] provides a comprehensive listing of properties to consider when observing any fuel type. This includes:

- Minimal fuel cost
- Adequate thermal conductivity
- Resistance to thermal cycling

- Adequate corrosion resistance
- Capable of quickly transmitting heat from center
- High neutron capture cross sections
- Capable of sustaining mechanical stresses
- Must be amenable for reprocessing and disposal

With regards to the project and its constraints, the focus on fuels was placed on a couple of the factors listed. Along the lines of consideration for the neutron capture cross sections was the purity of the fuels. In other words, utilization of fuels which are relatively free of constituent elements. This purity is with regards to something known as the heavy metal density within each material: with heavy metal referring to the higher-level actinides like uranium, plutonium, and thorium. Calculation of the heavy metal density is displayed in the equations 1-3. [9] Uranium nitride is used as an example in this process.

$$total\ molar\ mass\ of\ compound = m_U + m_N = m_{UN} \tag{1}$$

$$molar\ ratio\ for\ heavy\ metal = \frac{m_U}{m_{UN}} \tag{2}$$

$$heavy\ metal\ density = \rho_{UN} * \frac{m_U}{m_{UN}} \tag{3}$$

theoretical density of fuel = ρ_{UN}

molar mass of uranium = m_U

molar mass of nitrogen = m_N

Heavy metal isotopes have an influence on neutron economy through their reaction to neutron bombardment; and are divided into three categories. Fissile material is composed of the isotopes which undergo fission following capture of a thermal neutron. Familiar fissile isotopes include U-235, Pu-239, and Pu-241. Fertile material consists of isotopes that are not fissionable by thermal neutrons but can be converted into fissile isotopes: with some of the most known isotopes being U-238 and Th-232. Fissionable material is capable of undergoing fission after capturing either a fast neutron or thermal neutron. This includes isotopes like U-238, U-235, and Pu-240. Of relevance is the amount of fissionable material: which is found using the heavy metal calculation mentioned. Approximate heavy metal densities, along with their theoretical densities, for each fuel type are displayed in Figure 2.1.

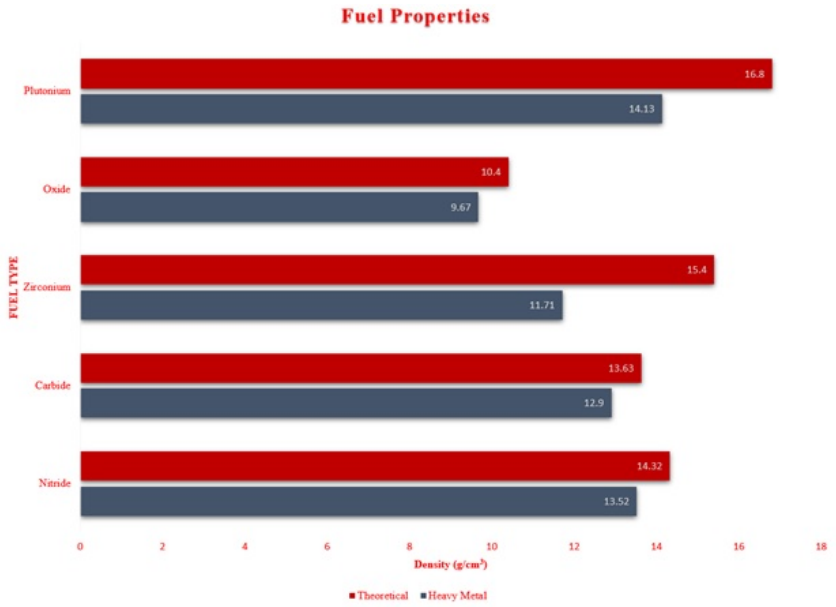

Figure 2.1: Fuel Density Data

Outside of heavy metal density, factors that can affect the neutron economy include enrichment values. It's important to clarify that U-238, while capable of undergoing fission directly under a fast neutron spectrum (1 MeV – 20 MeV), it is still multiple orders of magnitude less efficient than U-235 fission. This is pictured in the graphs for fission cross sections available in Figure 2.2.

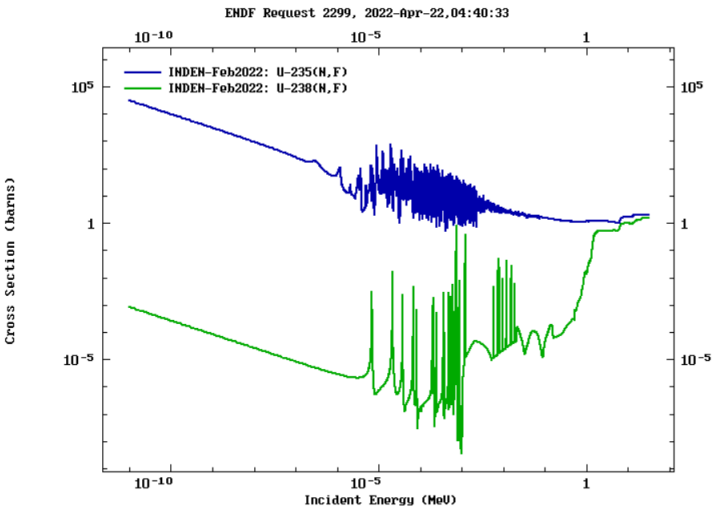

Figure 2.2: U-235 and U-238 Fission Cross Sections

Originally, the Versatile Test Reactor operated on U-PU-10Zr [17]. This is generally known as either plutonium or metallic fuel. Plutonium fuel is desirable due to the increased rate of fission following neutron capture compared to uranium fuel. While it does produce more neutrons per interaction, the downside of plutonium is that it does not occur naturally. Plutonium is mainly produced by the reprocessing of spent fuels; and it is also found to present itself during the operation of commercial nuclear power plants: usually as a result of neutron capture by U-238. It also has the added benefit of allowing for constant reactivity through the operation of Pu-240 as a burnable poison in the core. Due to supply issues, it is not considered within the confines of this project; but it is important to recognize the optimal performance exhibited by this fuel type.

Uranium Zirconium is one of the many metallic fuels utilized during earlier developmental stages of nuclear reactors. Notable examples of reactors that performed testing on this fuel type include EBR-II and the FTFF. Metallic fuels typically have high thermal conductivity, high fissile density, and low costs. It also carries high fissile and fertile densities to accompany its ease of fabrication. A major drawback noted by many researchers was the dimensional changes that can occur during usage. This has an adverse effect on the thermal conductivity of the fuel and can shorten its lifetime in the reactor due to the possibility of breaches. [Cochran] As noted by Crawford, these breaches can release of considerable amounts of fuel into the coolant could increase the radionuclide content of the primary system to unacceptable levels or could even perturb flow in coolant channels, thereby affecting other fuel rods in what is termed propagation of failure.

Uranium oxide, uranium carbide, and uranium nitride are all within a category known as ceramic fuels. While brittle, they are known to have some advantages over metal fuels. Two key issues mentioned by Murty [16] are the central fuel melting temperature of metal fuels and the excessive deformation due to irradiation instability at higher temperatures: this entails effects like creep deformation and irradiation swelling. Ceramic fuels dominate in three areas of interest:

- Operating temperatures
- Irradiation stability
- Corrosion resistance

Early on in the nuclear industry, uranium dioxide found itself chosen for commercial reactor use due to oxygen's low thermal neutron cross section.: preventing a serious loss of neutrons. It also doesn't have an interaction with the light water reactor coolant. While its low thermal conductivity is unappealing, the high melting point of oxide fuel allows for it to be utilized at high temperature. The most promising feature of uranium dioxide is the various fabrication methods available: leading to solutions which mitigate irradiation effects on the fuel. These irradiation effects are relevant due to phenomena like fuel swelling. This is an increased size in the fuel due to interstitials being introduced by neutron interactions. Eventually, this could lead to fuel failure: defined by the release of fission products into the coolant. Fuels like uranium monocarbide a uranium nitride have undergone research as replacements for oxide fuel due to the increased theoretical density mitigating irradiation damage.

Uranium carbide is found in the forms UC, U_2C_3, and U_2C. According to Murty [16], carbide fuel is considered ideal in comparison to metallic uranium and UO2 due to:

- Not undergoing a phase change until its melting point
- High uranium density
- Higher thermal conductivity than (UO_2)

Due to this higher uranium content and thermal conductivity, larger sizes for fuel elements can be achieved along with a higher power density and smaller primary components. Unfortunately, there are some significant disadvantages in using carbide fuel. The most significant is the fabrication process' complications: which lead to excessive costs and difficulties moving from a laboratory setting to an industrial setting. Of these, oxidation stability is notable due to it affecting the purity of the carbide fuel: leading to noticeable shifts in thermal properties. Uranium nitride provides similar benefits to carbide fuel; but its fabrication

process does not suffer from the lack of oxidation stability. In addition to this, it has a higher heavy metal density and thermal conductivity than carbide fuel. One issue that it does suffer from is the requirement to enrich the nitrogen. Due to the formation of C-14 from N-14, the nitrogen component must be highly enriched in N-15 to increase neutron economy. While infrastructure would need to be put in place for this, the nitrogen enrichment costs is expected to be offset by the lower uranium enrichment.

3 Economics of Design

3.1 Costs Associated with Reactor Design

A relevant aspect of design considerations is the overall cost for implementing a design (See Figure 3.1). The costs associated with a nuclear power plant are divided into three categories [21]:

- Capital Cost
- Operating Cost
- External Cost

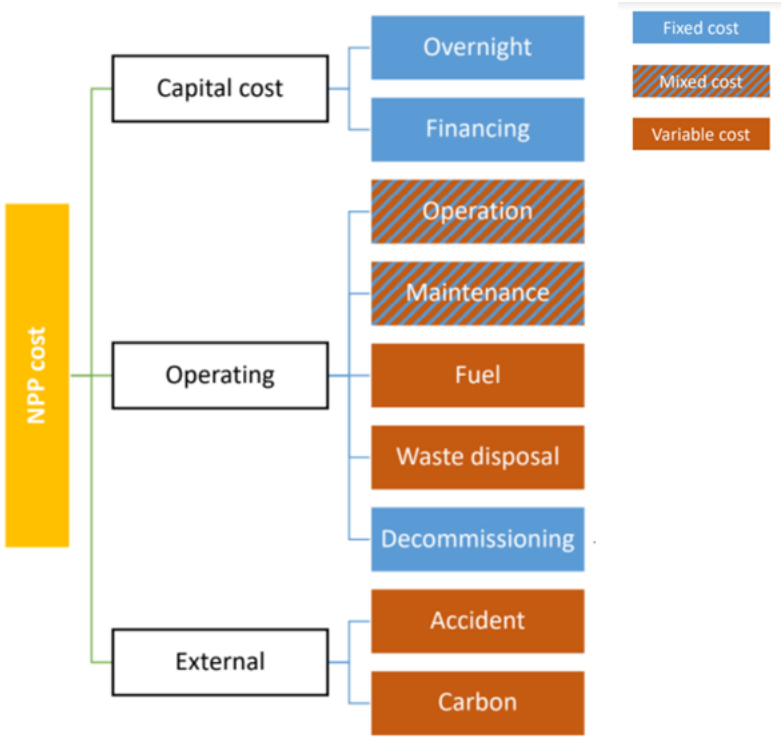

Figure 3.1: Nuclear Power Plant Cost Schematic

The capital cost is the largest percentage of the reactor costs. It represents the building and financing of nuclear power plants. These values are typically fixed prior to construction and might increase due to the delays that commonly

occur. The operating costs include everything from the payment and training of employees to the development of fuels for reactor operations. External costs are associated with accidents that might occur during operations.

3.2 Costs Associated with the Project

Under the circumstances provided by this project, the relevant aspect for economic analysis is the fuel. The costs associated with it, known as the front-end costs, are all speculative due to a reliance on supplier input. This front-end portion of the fuel cycle is made of the following components:

- Uranium Milling and Mining
- Uranium Conversion
- Uranium Enrichment
- Uranium Fuel Fabrication

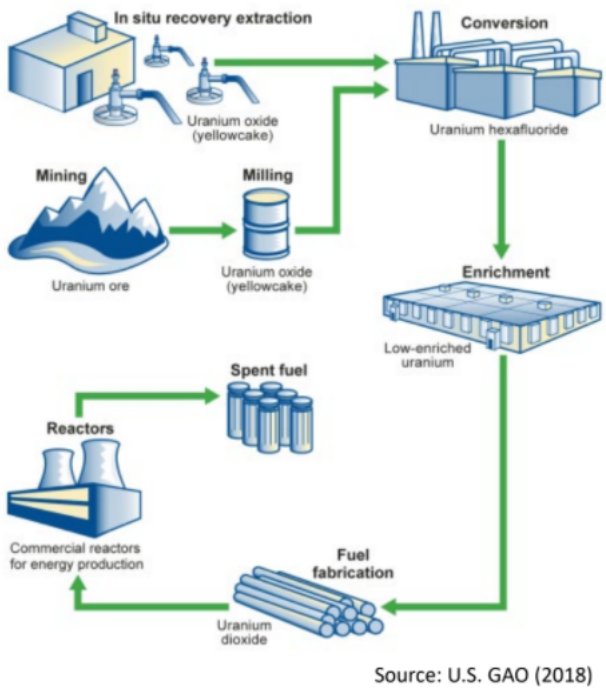

Figure 3.2: Nuclear Fuel Cycle

Uranium mining is the process of removing uranium ore from the earth along with the physical and chemical processing required in order to develop "yellowcake" uranium concentrate (U_3O_8). These reserves of uranium ore are not treated equally: as the quality is evaluated in the development of a recovery cost. Uranium is given a grade and recovery rate in combination with the mining cost: in which the grade is the average percent of U_3O_8 per ton of ore.

Uranium conversion comes as the next step in the process. Its purpose is to turn uranium into a gaseous state for enrichment and purify the uranium to a greater extent than it was in the milling stage. This produces the mono-isotopic gas UF_6. The gas is then cooled to a solid and transported to enrichment plants.

The enrichment process is meant to increase the U235 isotopic content from the natural value of 0.711 $wt\%$ to a value required by the reactor in question. While typically at a value around 5% for light-water reactors, the Versatile Test Reactor will function between the $5 - 20\%$ enrichment range. The enrichment capacity is measured in terms of separative work units (SWU). SWU is best described as an indication of energy consumption as a function of the amount of uranium processed, the degree to which it is enriched, and the level of depletion of the remainder. The remainder is known as the tails or waste.

Fuel fabrication is the most unique aspect of cost analysis with its dependence on reactor type. The case of uranium dioxide is most familiar: as this is the fuel utilized by LWRs. Here, the incoming UF_6 is used to produce UO_2 powder. This powder is then processed in order to manufacture pellets; and these are placed into fuel rods to create the final fuel assembly structure.

3.3 Costs Associated with each Design

In the original design, the associated fuel cost, while not given, can be approximated at $728 million - $1.6 billion. This number is generated from the typical 28% portion [4] that is considered to be the fuel cost and the range of $2.6 - $5.8 billion price tag of the Versatile Test Reactor[17]. While the true numbers related to each aspect of costs are not provided, it is possible to use a combination of mass balance equations and given data to determine the approximate annual cost of the fuel cycle. It's important to note that the method considered in the enrichment process is gaseous diffusion: as the usage of laser enrichment is not commercially available and therefore unlikely to be utilized.

The external variables considered in gaseous diffusion must satisfy the following mass-balance equations:

$$F = P + W \tag{4}$$

$$x_f F = x_p P + x_w W \tag{5}$$

x_f = weight fraction of U-235 in the feed

x_p = weight fraction of U-235 in the fuel

x_w = weight fraction of U-235 in the waste stream

F = mass of feed material

P = mass of product material

W = mass of waste material

The weight fraction in the feed is the natural enrichment of uranium at any period of time. The weight fraction in the fuel is simply the percentage enrichment desired for the reactor, and the waste stream enrichment is something that is decided by the manufacturer. As this is not provided, the assumed value for waste enrichment is 2.5% due to the United States producing a value between 2% and 3% for the waste stream.

From each enrichment it becomes possible to calculate what are known as separation potentials. In the case of any enrichment value, the following equation [4] may be used.

$$V(x_i) = (2x_i - 1)\ln(\frac{x_i}{1 - x_i}) \tag{6}$$

i = p,f,w

From these separation potentials, the amount of separative work units may be calculated. As opposed to directly finding SWU, a component known as the SWU factor can be used at times. It has units of SWU/kg-U.

$$SWU = P * V(x_p) + W * V(x_w) - F * V(x_f) \tag{7}$$

$$SF = SWU/P \tag{8}$$

The pricing of natural uranium and the cost of conversion are provided along with the price of SWU. The values for each were extracted from UxC and displayed in Figure 3.3. These values are updated each month.

	1 US$ =		0.87841 €‡	
Ux U_3O_8 Price® (lb)	**$47.25**	**(+3.25)**	**€41.50**	**(+2.85)**

Month-End Ux Prices as of October 25, 2021

[Change from previous month]

	1 US$ =		0.86117 €‡	
Ux U_3O_8 Price® (lb)	**$47.40**	**(+4.40)**	**€40.82**	**(+3.79)**
Ux NA Conversion Price (kgU)	**$15.75**	**(-0.25)**	**€13.56**	**(-0.22)**
Ux EU Conversion Price (kgU)	**$15.75**	**(-0.25)**	**€13.56**	**(-0.22)**
Ux NA UF_6 Price (kgU)	**$137.50**	**(+11.50)**	**€118.41**	**(+9.90)**
Ux NA UF_6 Value§ (kgU)	*$139.60*	*(+11.25)*	*€120.22*	*(+9.69)*
Ux EU UF_6 Value§ (kgU)	*$139.60*	*(+11.25)*	*€120.22*	*(+9.69)*
Ux SWU Price (SWU)	**$56.00**	**(+0.50)**	**€48.23**	**(+0.43)**

Figure 3.3: UxC Front-End Fuel Cycle Pricing

By totaling these, a value can be found for the price of enrichment using the following formula [4].

$$PE = (PU + PC) * (F/P) + PS * SF \tag{9}$$

The final calculation factor, fabrication, was not directly available. Using multiple data sources, these numbers were able to be calculated. These values and the sources utilized are displayed in Table 1. Using all of this accumulated data, it becomes possible to determine the front-end cost of the fuel.

Fuel Type	Cost per Unit	Source
U-10Zr	$391.20/kgU	Judkins & Olsen [13]
UO2	$274/kgU	UxC [22]
UC	$503.61/kgU	Judkins & Olsen [3]
UN	$500/kgU	Khaldoon Al-Dawood [1]

Table 1: Fuel Fabrication Pricing

While the different fuel types have varying properties as a result of their chemical makeup, the method for obtaining the pricing of each is similar. Each fuel has a theoretical density. Using this, along with the volume of the fuel provided by specifications, lead to a mass of the compound which is present in the core. Next is the calculation of the molar mass of uranium within the core. For simplicity, the assumption is that the element is strictly divided into the isotopes U235 and U238. Equation 10 was utilized for this.

$$\frac{1}{M_U} = \frac{w_{25}}{M_{25}} + \frac{w_{28}}{M_{28}} \tag{10}$$

After receiving a molar mass for uranium, the ideal molar mass of the corresponding element is used. This value is extracted from the Chart of the Nuclides[19]. The molar mass values are then combined to produce a total molar mass for the fuel. This value is then shifted into a ratio between uranium and the total. It is then multiplied by the total mass in order to obtain the mass of uranium available in the product.

With the product mass available, there are two unknowns to be solved by the two mass balance equations provided previously. This gives an amount of material available for SWU, natural uranium, and conversion. These values are multiplied by the cost factors provided by UxC to produce a final price for the product during each fuel cycle.

3.4 Levelized Cost of Fuel

A concept that was introduced during research on fuel cycle cost is that of levelized cost of electricity (LCOE). This is a tool which takes the fixed an variable costs and combines them for a simplified analysis; and it is best described as a measurement of the net present cost of electricity generation over a lifetime. Often, it is displayed in units of $/MWh. In the case of HALEU fuel in particular, Carlson [3] explains that cost is best analyzed in terms of a value that is quite similar to this: the levelized cost of fuel (LCOF). This can be presented by looking at the differences between scenarios in which a uniform core of uranium oxide fuel is observed.

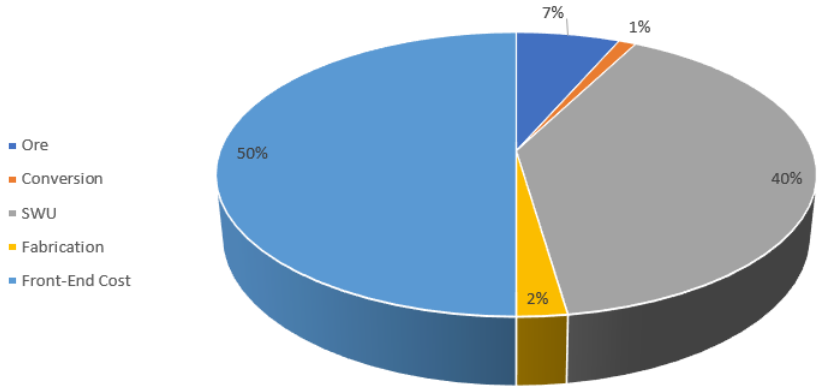

Figure 3.4: 4% Enriched Fuel Percents

Component	Cost
Ore	$5,553,520.27
Conversion	$937,316.25
SWU	$33,991,764.28
Fabrication	$1,973,269.41
Front-End Cost	$42,455,870.20

Table 2: 4% Enriched Fuel Cost Breakdown

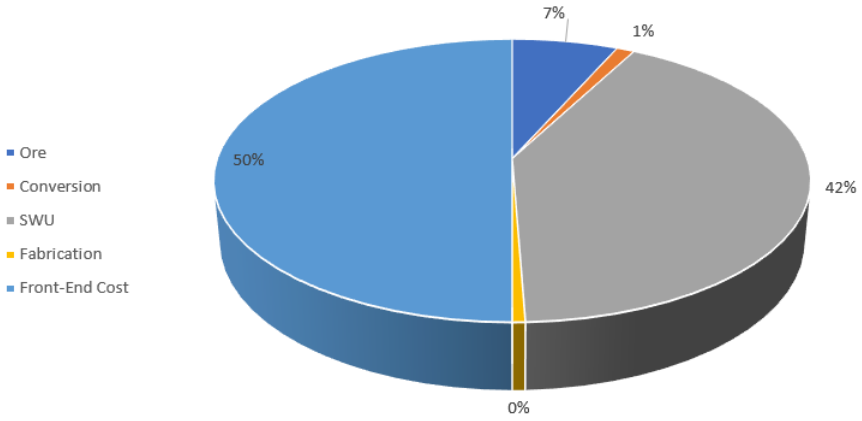

Figure 3.5: 15% Enriched Fuel Percents

Component	Cost
Ore	$21,843,846.38
Conversion	$3,686,777.24
SWU	$136,576,220.14
Fabrication	$1,973,269.41
Front-End Cost	$164,080,113.17

Table 3: 15% Enriched Fuel Cost Breakdown

In looking at the front-end fuel cycle cost for the Versatile Test Reactor under a uniform core of uranium oxide fuel, a clear difference in the percentage of costs occupied by separative work units. In the case of a 4% enrichment value, the cost of enrichment occupies a much lower value than that of a 15% enrichment of uranium. In addition, the total costs of fuel increase drastically.

For calculating the levelized cost of fuel, the method is presented in the following equations [3]:

$$C_U = C_{ore} + C_{conversion} + C_{SWU} + C_{fabrication} \tag{11}$$

$$LCOF = \frac{C_U}{P * T_{EFPD}} = \frac{C_U}{P * \eta * T_{cycle}} \tag{12}$$

C_U = Cost of Loading

P = Power Generated

T_{EFPD} = Effective Full Power Days

T_{cycle} = Fuel Cycle Length

η = Capacity Factor

4 LUPINE

The bulk of this project involved designing the uranium core and testing different designs, examining the resulting outputs, and checking if they met the specifications. This was done using the computer code LUPINE. The different aspects of LUPINE will be summarized in this section.

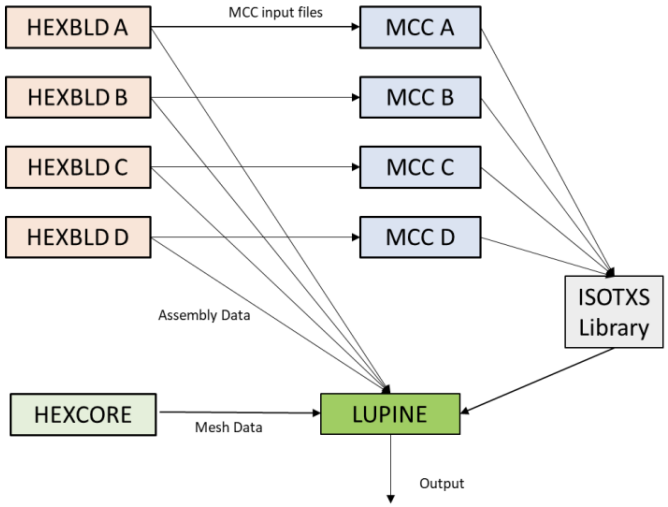

Figure 4.1: Workflow of LUPINE

4.1 HEXBLD

The first step in running LUPINE is HEXBLD. This preprocessor allows for geometrical and material inputs to define the bundles. A bundle for each individual assembly type, control rod, safety rod, fuel assembly, shield, axial reflector, radial reflector, and experiment guide tube, is required. This step takes all of the inputs and smears all of the data by volume fraction to radially homogenize it. The HEXBLD data will then be sent to both MCC, which will compute all of the cross sections for the materials, and the final step of LUPINE, which will solve the multiphysics. The inputs and descriptions are provided in the Table 4.

Variable	Description
npins	number of fuel pins in assembly
dwrap	diameter of wire wrap
rpitch	rod pitch
hsize	channel can size
boxth	channel thickness
apitch	assembly pitch
hsize2	channel can size of inner channel
boxth2	channel thickness of inner channel
coolant	coolant type
fuel_type	fuel type
enrich	fuel enrichment of u235
Nenrich	N-15 enrichment
porosity	nitride porosity
gap_type	gap type
clad_type	clad type
thexp	turn thermal expansion on
thexp_clad	thermal expansion coefficient for clad
thexp_crod	thermal expansion coefficient for control rod
thexp_fuel	thermal expansion coefficient for the fuel
temp_cool	temperature of coolant
temp_crod	temperature of control rod material
temp_clad	temperature of clad material
temp_fuel	temperature of fuel material
temp_bgap	temperature of gap material
den_cool	density of coolant material
den_crod	density of control rod material
den_clad	density of cladding material
den_fuel	density of fuel material
den_bgap	density of gap material
ifburn	add burnup isotopes
ifmcnp	create MCNP file
ifserp	create Serpent file
isoset	use predefined set of fuel isotopes for burnup calculations
include	file name to read additional input from
pinmat	rod materials for different radial regions
pinrad	rod radii for different radial regions

Table 4: HXBLD Inputs

4.2 MCC

Using the HEXBLD data, MCC is utilized to generate the microscopic cross sections for the assembly. MCC will produce a unique ISOTXS file for each

assembly. These files will then need to be merged into a single ISOTXS file which is an input for the file step of LUPINE. The cross sections are necessary for LUPINE to be able to interpolate at different temperatures.

4.3 HEXCORE

In Hexbld, the 2D geometry of each assembly is defined, in Hexcore, these 2D inputs are arranged in a radial mesh and then the axial mesh is specified as well to delineate the 3D model. Just like HEXBLD, this step in the LUPINE process is defined by hexagonal geometry. In building the 3D Core, the position of each assembly must be designated for the radial mesh. Starting in the center assembly in the core, defined as ring 1, each step out towards the edge of the core will increase the ring number, with the final step being ring 11. Within each ring, the specific position of the assembly is also defined by a number, starting at one and increasing in a counter clockwise direction until the starting position is reached. The axial position of each assembly is important in constructing the 3D core. These inputs will decide the height of each assembly as well as allow for the composition of fuel rods that are made up of multiple sections, i.e., fuel pins surrounded on the top and bottom by a fission gas plenum and shield. The output of HEXCORE can be used in the final step, LUPINE.

4.4 LUPINE

LUPINE is the final step in running the code. It takes all of the inputs from HEXBLD, HEXCORE and MCC to solve the multi-group neutron transport equation. It takes into account radial heat conduction to calculate the surface temperatures of the clad, the fuel as well as the fuel centerline and can determine the average temperatures, axial heat convection, thermal expansion from leakage and density effects, and the cross section interpolations for the coolant, clad and fuel at different temperatures. Many properties needed for this trade study are built into LUPINE including, the different types of fuel, the structural materials and the sodium coolant. Depletion of the core is an important aspect of this study and can be analyzed with LUPINE, which uses Chebyshev Rational Approximation. 20 actinides and 80 fission products are included in the code; part of the decay chain is shown in Figure 4.2.

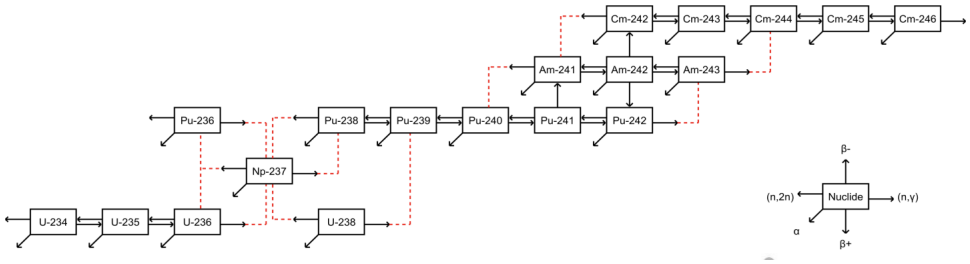

Figure 4.2: LUPINE Depletion Chain

5 Designs

5.1 Geometries

The VTR is a hexagonal core design, which increases the packing factor that is required for fast reactors due to the high leakage, and contains 331 assemblies. Figure 5.1 is a layout of one potential core. These assemblies are a combination of fuel assemblies, control rods, safety rods, experimental guide tubes, reflector assemblies and shield assemblies. These assemblies will be described in detail by the figure.

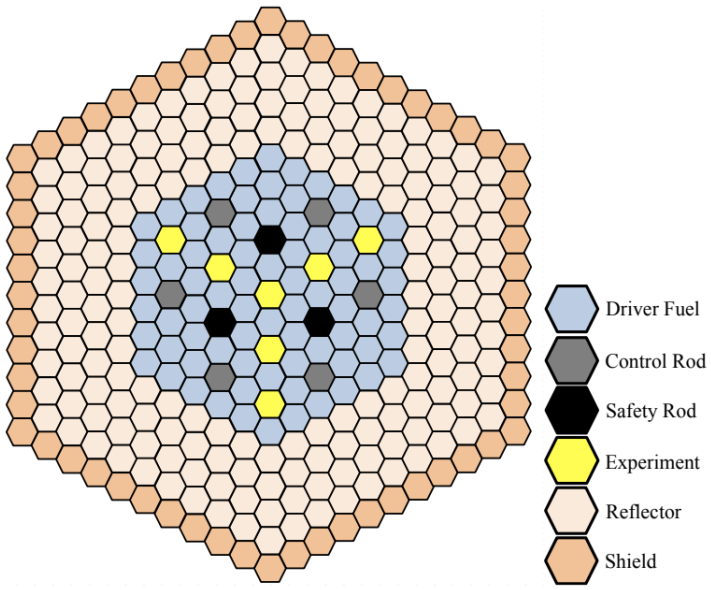

Figure 5.1: Potential VTR Core Layout

5.2 Assemblies

The number of fuel assemblies varies between tests but the assembly design itself remains relatively standard between the different fuel types and core designs. Axially, each fuel assembly is made up of a reflector (50 cm in length), followed by the active fuel (between 60 to 100 cm in length), and then the fission gas plenum (the same length as the fuel) and finally another reflector.

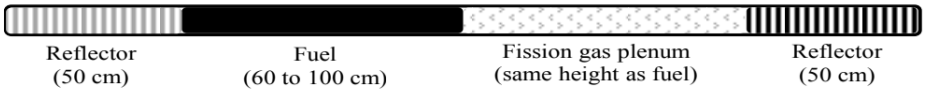

Figure 5.2: Axial Visualization of a Fuel Assembly

Radially, the fuel assembly will be surrounded by coolant, liquid sodium, and a cladding of HT9 steel (thickness?). Within the cladding there will be 271 fuel pins, which contain the uranium fuel surrounded by an HT9 cladding and a wire wrap which acts as a spacer grid to keep the fuel pins evenly distributed, with coolant running in between them.

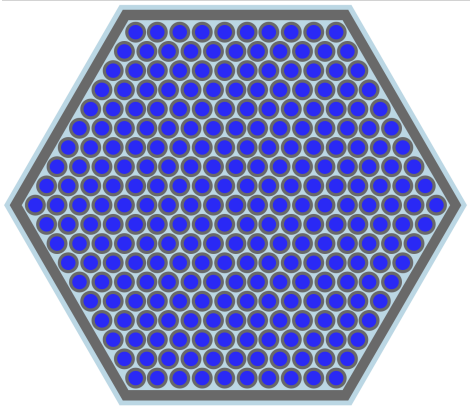

Figure 5.3: Radial Visualization of a Fuel Assembly

There are 6 control rods and 3 safety rods in a standard core design. Both the control and safety rods are modeled the same way and utilize enriched B4C as the absorber .Similar to the fuel assembly, a wire wrap made of HT9 will be used as a spacer grid. Between the rods, there will be coolant which will then be surrounded by an inner cladding. In the small space between the inner and outer claddings, there is a gap for sodium coolant.

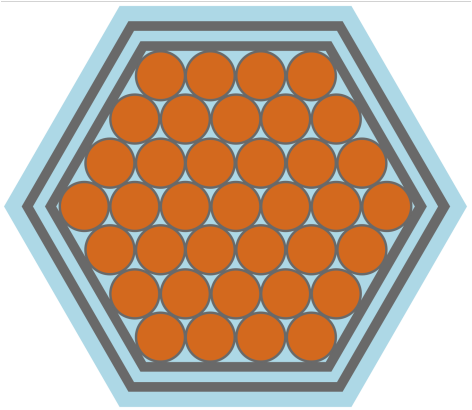

Figure 5.4: Radial Visualization of a Control Rod Assembly

The reflectors are modeled as pins of HT9 with coolant running between them which are then surrounded by a cladding, also made of HT9.

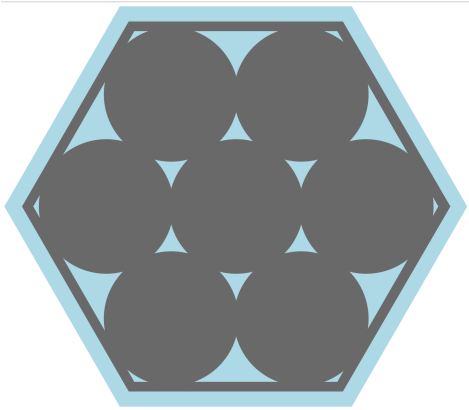

Figure 5.5: Radial Visualization of a Reflector Assembly

Finally, the shield assemblies are rods of enriched B_4C which are surrounded by a small gap of bond gas, in our case helium, which allows for thermal expansion of the rods, and then a cladding of HT9. Between the rods, as in the previous designs, there is coolant and then the whole thing is surrounded by a cladding of HT9.

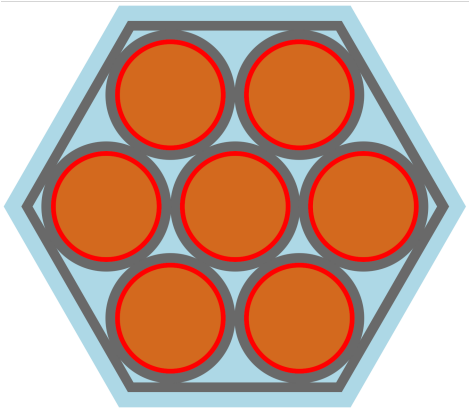

Figure 5.6: Radial Visualization of a Shield Assembly

6 Core Design

Prior to design was the creation of an initial core that modeled the Versatile Test Reactor's original design.

Our initial approach for design was picking a simple concept, a symmetrical core with only one type of fuel, metallic uranium, and designing all of the necessary components such as the shields, control rods, reflectors and fuel assemblies. We ran through each step of LUPINE, including HEXBLD, HEXCORE, MCC and LUPINE itself to get a working model and a result to draw conclusions from and compare to future designs. This core contained one ring of shields, 2 rings of reflectors, 9 control rods (including the safety rods), 4 experiment guide tubes and the rest 20% enriched metallic uranium fuel with an active fuel height of 80 cm. A visualization of the design is provided by Figure 6.1.

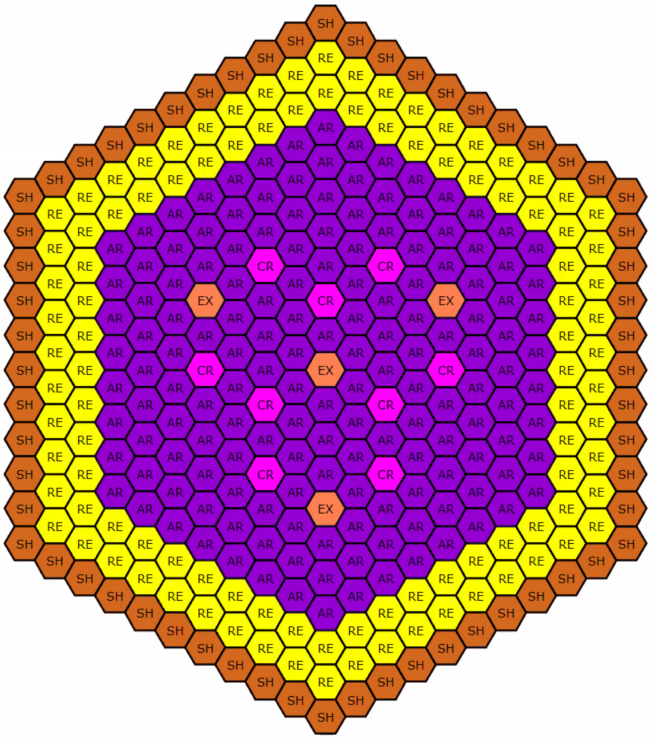

Figure 6.1: Initial Core Design

6.1 Preliminary Modifications

The design in Figure 6.1 results in a k_{eff} value of 0.987964. While this would not be a feasible final design due to the differing efficiencies between uranium and plutonium fuel, we used it to see what we needed to change in order to achieve a viable core. The next design contained a mix of fuel, uranium nitride, carbide and metallic, all enriched to 20%. This design attempted a more 'circular' loading pattern to potentially flatten the flux distribution near the edges of the core. It also placed metallic uranium fuel, the fuel with the highest density, right around the experiment tubes to make sure they were still receiving high levels of flux. The visualization of this new design is provided in Figure 6.2.

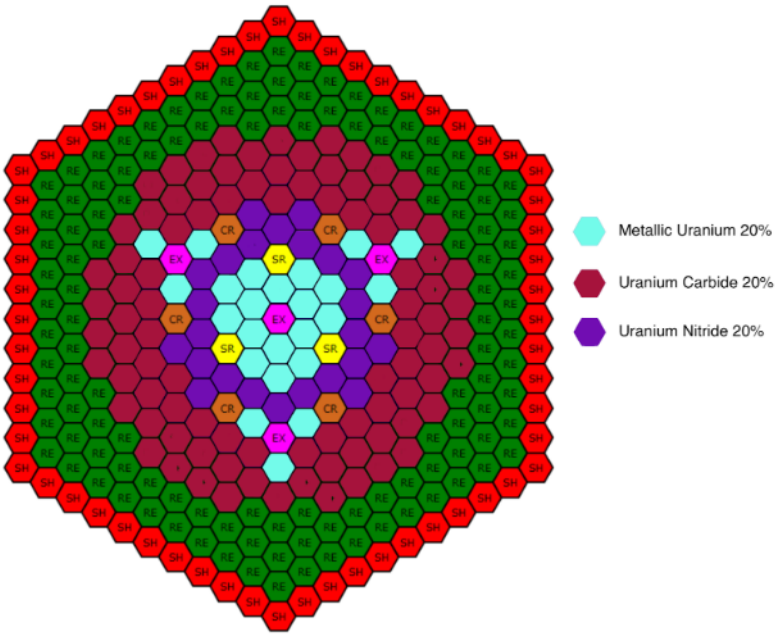

Figure 6.2: Circular Loading Pattern

Despite this core design failing to reach a fast flux value above 4.63E+11, an evaluation of the front-end cost for this core was performed. As noted in the economics section, the usage of higher enrichment vastly increases cost beyond what was expected of plutonium. It is also worth noting the increases that occur due to the reliance on newer fuel types with limited manufacturing infrastructure.

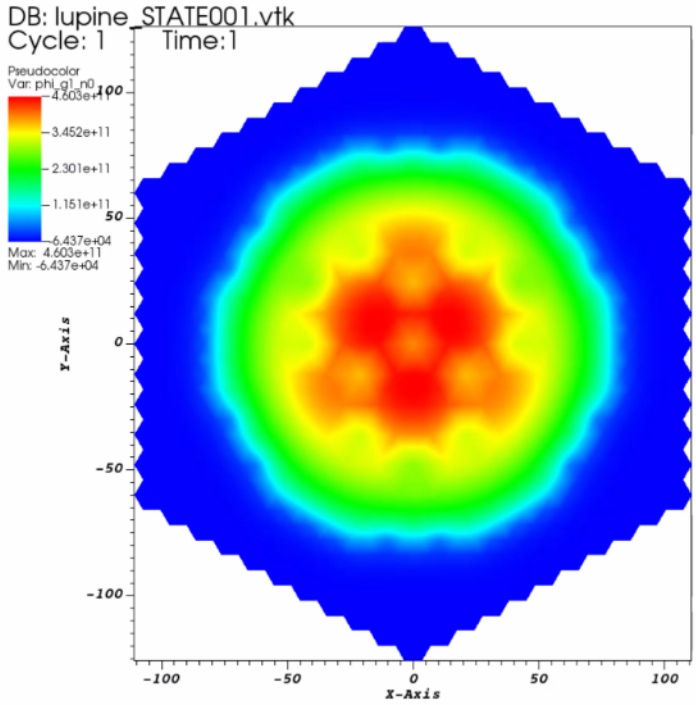

Figure 6.3: Circular Loading Pattern Flux Map

Fuel Type	Enrichment	Percent Composition	Total Fuel Cycle Cost
UN	20%	15.38%	$35,131,000.00
U-10Zr	20%	15.38%	$30,320,000.00
UO2	N/A	0.00%	$0.00
UC	20%	57.69%	$126,426,000.00
Total Cost			$191,877,000.00

Table 5: Circular Loading Pattern Cost Components

Fuel Type:	UN	Fuel Type:	U-10Zr
Ore	$4,646,257.12	Ore	$4,024,231.93
Conversion	$784,189.50	Conversion	$679,204.86
SWU	$29,128,046.26	SWU	$25,228,481.89
Fabrication	$572,011.65	Fabrication	$387,626.51
Front-End	$35,130,504.53	Front-End	$30,319,545.19
Fuel Type:	UO2	Fuel Type:	UC
Ore	$0.00	Ore	$16,718,708.24
Conversion	$0.00	Conversion	$2,821,762.80
SWU	$0.00	SWU	$104,811,958.07
Fabrication	$0.00	Fabrication	$2,073,140.29
Front-End	$0.00	Front-End	$126,425,569.39

Table 6: Circular Loading Pattern Cost Breakdown

6.2 Uniform Cores

While the fast flux was a concern for the core, another factor taken into account was the k-effective for each core tested. The reasoning behind this was that the core must not only reach a fast flux of 4E+15. It must also be able to reach the expected EFPD of 300 to the greatest extent possible. In other words, it must be capable of sustaining itself at the peak fast flux desired for an extended period of time. With this in mind, a new approach was taken in which the fuels were evaluated through their performance as a uniform core. Oxide fuel was excluded from this due to the heavy metal density indicating inferior performance.

Fuel Type	# Reflector Rings	k_{eff}
U-10Zr	3	0.947289
UN	3	0.93345
UC	3	0.945039
U-10Zr	2	0.988457
UN	2	0.97098
UC	2	0.984201
U-10Zr	1	1.015769
UN	1	0.99545
UC	1	1.00975

Table 7: Reflector Ring Reduction at 80 cm

In an attempt to reach the required parameters for reactor operation, the core's amount of reflector rings was shifted multiple times to see the effects of adding more fuel to the core. Three of the experimental ports were also removed: leaving a single experimental port in the middle of the core. This resulted in the increase of k_{eff} values in all scenarios alongside a shift from 156 fuel assemblies to 159 fuel assemblies in the core.

Fuel Type	# Reflector Rings	k_{eff}
MU	3	0.984225
UN	3	0.966393
UC	3	0.978952
MU	2	1.026559
UN	2	1.00476
UC	2	1.0191
MU	1	1.054916
UN	1	1.0303
UC	1	1.04565

Table 8: Reflector Ring Reduction at 100 cm

Further alterations were made to the design in the form of increased fuel heights: thereby adding more fuel to the core. This leads to an increase in k_{eff}.

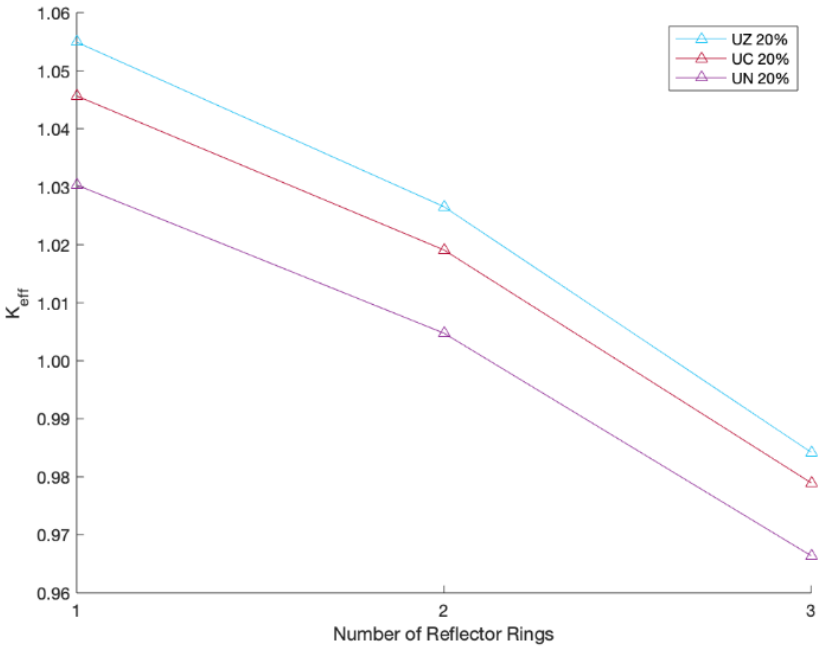

Figure 6.4: K-Effective and Reflector Ring Correlation

In looking to develop a focus on a certain fuel type, a uniform core of each fuel type was designed under the new design; and an economic analysis was performed in terms of the front-end fuel cycle cost. The flux maps for each type were also generated in order to evaluate any peaking that occurs in the core.

6.2.1 U-10Zr

Component	Cost
Ore	$33,325,670.65
Conversion	$5,624,665.27
SWU	$208,923,365.63
Fabrication	$3,210,032.07
Front-End Cost	$251,083,733.61

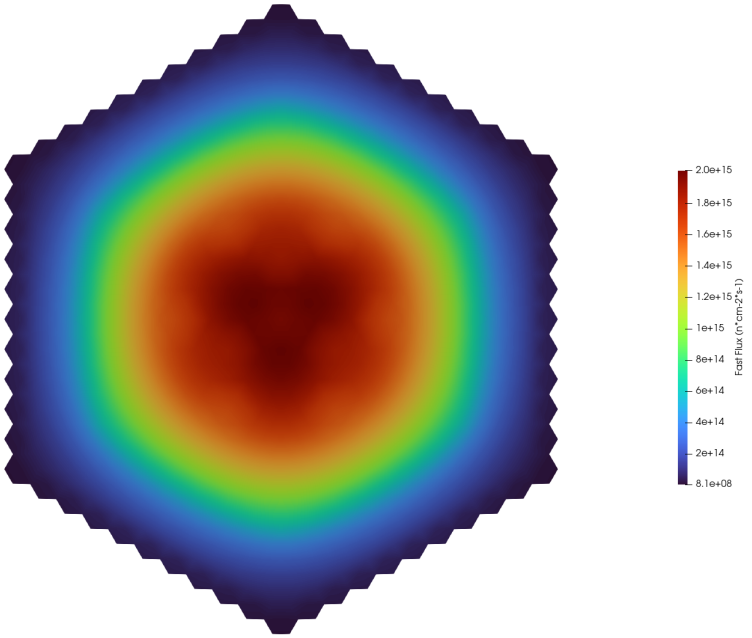

Figure 6.5: Metallic Fuel Flux Map

6.2.2 UO2

Component	Cost
Ore	$29,248,540.07
Conversion	$4,936,532.24
SWU	$183,363,254.60
Fabrication	$1,973,269.41
Front-End Cost	$219,521,596.32

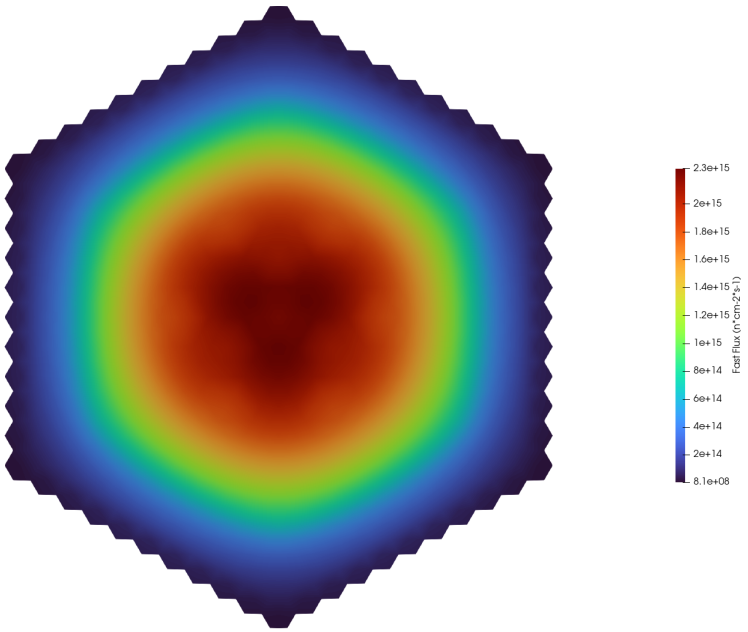

Figure 6.6: Oxide Fuel Flux Map

6.2.3 UC

Component	Cost
Ore	$36,920,480.70
Conversion	$6,231,392.84
SWU	$231,459,740.74
Fabrication	$4,578,184.80
Front-End Cost	$279,189,799.08

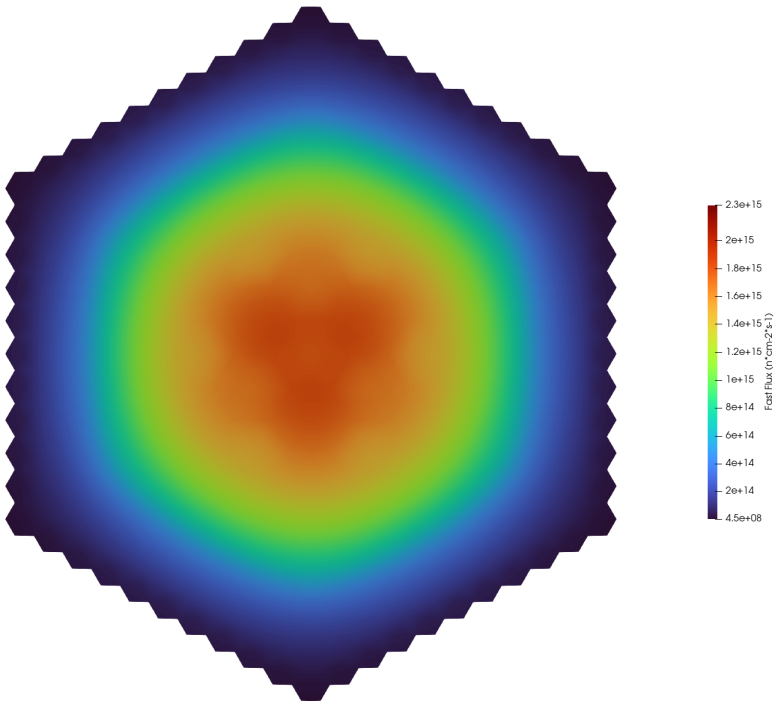

Figure 6.7: Carbide Fuel Flux Map

6.2.4 UN

Component	Cost
Ore	$38,476,816.82
Conversion	$6,494,069.32
SWU	$241,216,633.06
Fabrication	$4,736,971.45
Front-End	$290,924,490.64

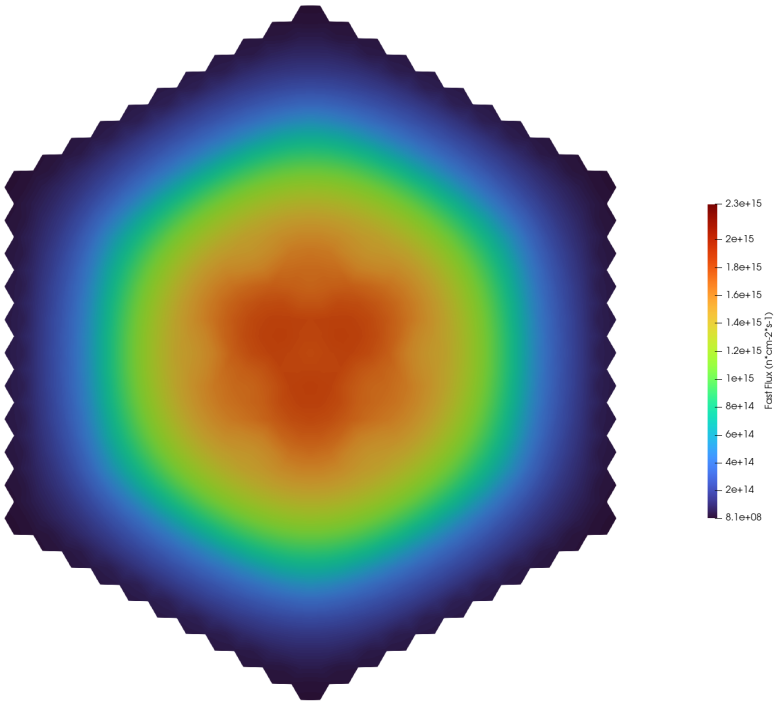

Figure 6.8: Nitride Fuel Flux Map

Fuel Type	k_{eff}	Peak Fast Flux	Front-End Cost
U-10Zr	1.02591	2.01E+15	$251,084,000
UO2	0.88667	2.28E+15	$219,522,000
UC	1.01357	1.84E+15	$279,190,000
UN	0.9985	1.85E+15	$290,924,000

Table 9: Uniform Core Performance Summary

6.3 In-Out Designs

The In-Out loading pattern is one available in Tsoulfanadis' text. [4] Their design is meant to provide a high thermal neutron flux alongside low leakage with one of the main downsides being unacceptable power peaking. The initial In-Out design concept is presented in Figure 6.9. In looking to determine which fuels were to be utilized, a binary core design was generated in place of the design displayed. The first case used a combination of U-10Zr and carbide fuel. This was followed with a combination of carbide and nitride fuel.

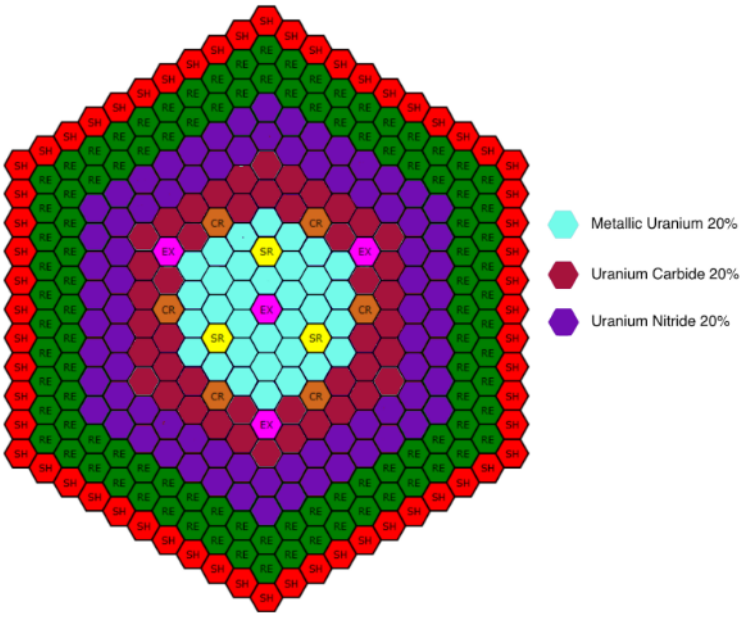

Figure 6.9: In-Out Design Concept

# Metallic Rings	# Carbide Rings	k_{eff}
0	8	1.01906
1	7	1.01906
2	6	1.01972
3	5	1.02084
4	4	1.02283
5	3	1.02421
6	2	1.02577
7	1	1.02661
8	0	1.02672

Table 10: In-Out Design w/ Metallic and Carbide Fuel

# Carbide Rings	# Nitride Rings	k_{eff}
0	8	1.00478
1	7	1.00478
2	6	1.00593
3	5	1.00771
4	4	1.01053
5	3	1.01256
6	2	1.01567
7	1	1.01816
8	0	1.01906

Table 11: In-Out Design w/ Nitride and Carbide Fuel

In observing the data presented by Table 7 and Table 8, it was noted that the carbide fuel led to an increased k_{eff} in the core. Due to this, further investigation into the potential of this fuel in the newly designed core was performed.

6.4 Checkers Pattern

Another method proposed by the literature was the idea of scatter loading. This is also known as the checkerboard pattern. In utilizing this, it is possible to achieve uniform power distribution. With metallic fuel providing the greatest level of performance, a mixture of loading patterns utilizing U-10Zr as a base were designed. Three of these designs are presented under the classification of Checkerboard-1, Checkerboard-2, and Checkerboard-3.

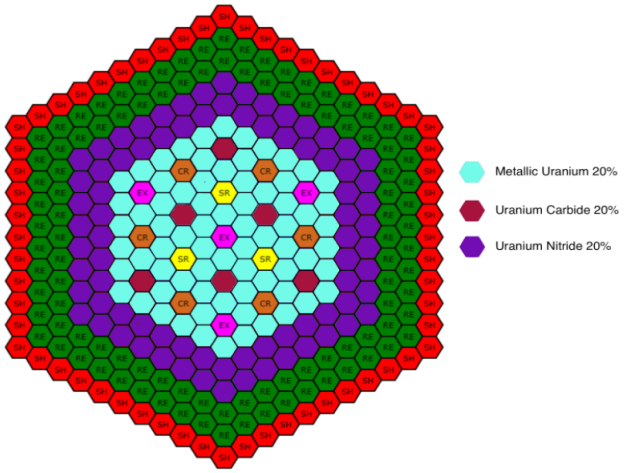

Figure 6.10: Checkerboard-1

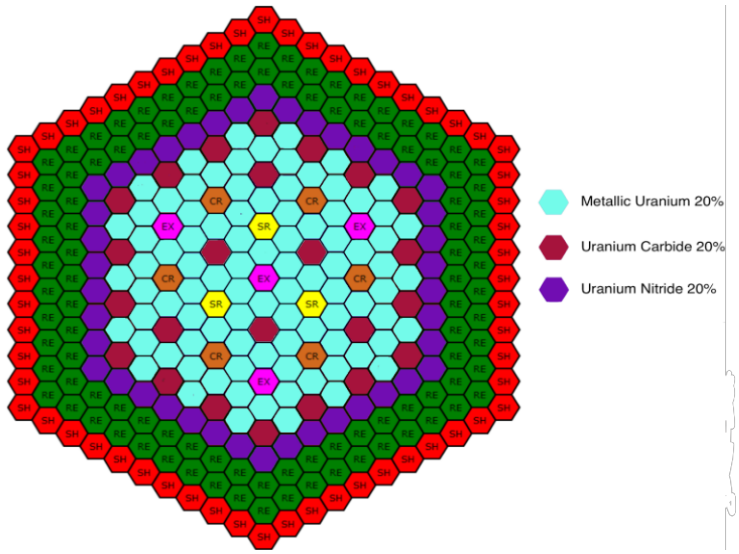

Figure 6.11: Checkerboard-2

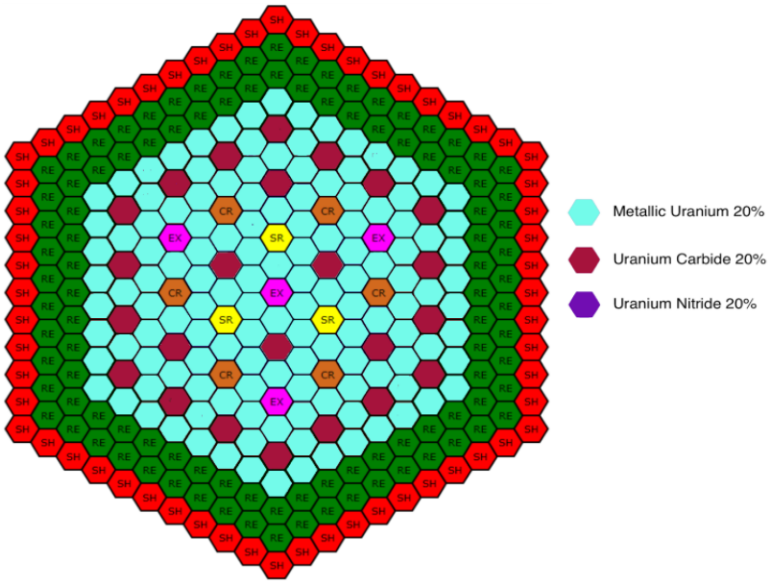

Figure 6.12: Checkerboard-3

The first noticeable indication that the mixed fuel design could improve the viability of the reactor was observed after the following design, Checkerboard-3,

resulted in a k_{eff} that was higher than that of a single fuel reactor containing metallic uranium, the fuel with the highest uranium density.

Design	k_{eff}	k_{eff} (Burnup)
Checkerboard-1	1.03273	1.03272
Checkerboard-2	1.03561	1.03560
Checkerboard-3	1.03679	1.03680

Table 12: Checkerboard Design k_{eff} Values

The k_{eff} values, both before and after burnup were introduced into the code and are shown in the Table 9 for each checker loading pattern case. This design was our most effective case, with Checkerboard-3 obtaining a k_{eff} of 1.03679 with 2 rings of reflectors while the design with only metallic uranium and 2 reflector rings only had a k_{eff} of 1.026559. We believed that this type of loading pattern will be able to be improved even more and further investigation into this design was completed following an analysis of its base state.

Fuel Type	Enrichment	Percent Composition	Total Fuel Cycle Cost
UN	20%	0.00%	$0.00
U-10Zr	20%	83.02%	$208,447,000.00
UO2	20%	0.00%	$0.00
UC	20%	16.98%	$47,410,000.00
Total Cost:			$255,857,000.00

Table 13: Checkerboard-3 Cost

Fuel Type:	UN	Fuel Type:	U-10Zr
Ore	$0.00	Ore	$27,666,594.50
Conversion	$0.00	Conversion	$4,669,533.43
SWU	$0.00	SWU	$173,445,812.98
Fabrication	$0.00	Fabrication	$2,664,932.28
Front-End	$0.00	Front-End	$208,446,873.19
Fuel Type:	UO2	Fuel Type:	UC
Ore	$0.00	Ore	$6,269,515.59
Conversion	$0.00	Conversion	$1,058,161.05
SWU	$0.00	SWU	$39,304,484.28
Fabrication	$0.00	Fabrication	$777,427.61
Front-End	$0.00	Front-End	$47,409,588.52

Table 14: Checkerboard-3 Cost Breakdown

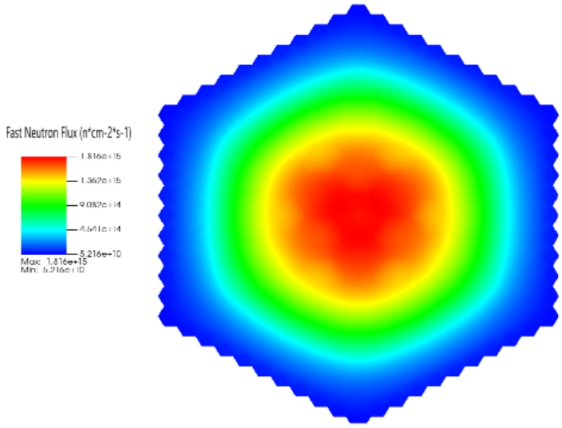

Figure 6.13: Checkerboard-3 Flux Map

To further investigate the reason the addition of uranium carbide to the system resulted in an increase in k_{eff}, and to find an optimal core design from this mixed fuel method, the following systematic approach was utilized. First, the design aspects we want to compare are the k_{eff} as previously mentioned, the peak fast flux in the center of the core, the effects of depletion (i.e., the projected length of a fuel cycle) as well as the total cost of the fuel per cycle. Next, the following designs were tested and compared such that a conclusion could be drawn regarding the effects of uranium carbide and metallic uranium mixed fuels.

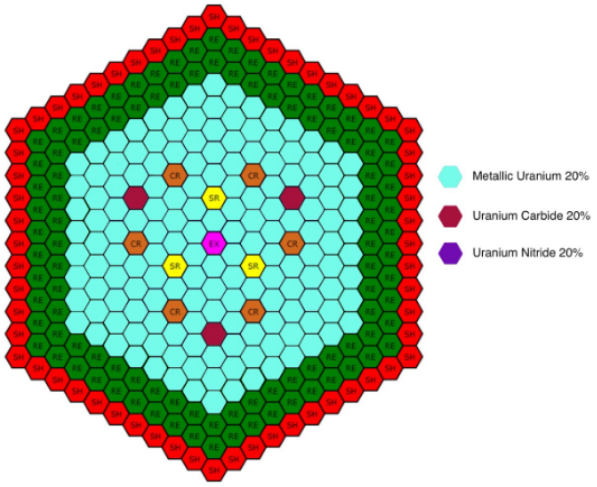

Figure 6.14: Carbide Insertion Design A

Design	Peak Fast Flux	k_{eff}	# of Carbide FA	Front-End Cost
A	2.03E+15	1.02313	3	$251,614,000.00
B	2.03E+15	1.02302	6	$252,144,000.00
C	2.01E+15	1.02255	9	$252,674,000.00
D	2.01E+15	1.02225	12	$253,205,000.00
E	2.00E+15	1.02214	15	$253,736,000.00
F	2.00E+15	1.02192	19	$254,442,000.00
G	1.99E+15	1.02415	23	$255,149,000.00
H	2.00E+15	1.0215	27	$255,857,000.00

Table 15: Carbide Insertion Test Results

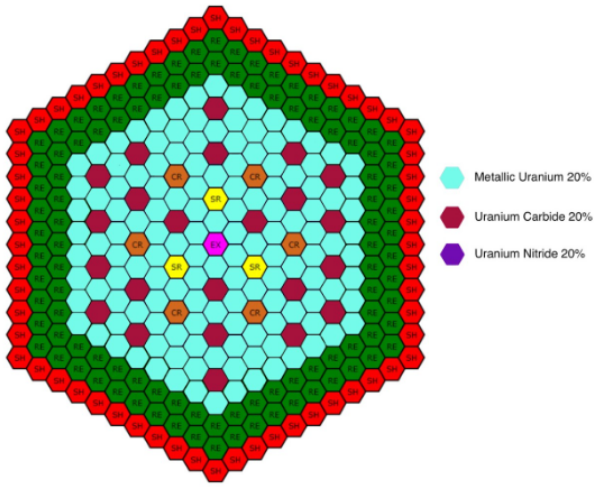

Figure 6.15: Carbide Insertion Design B

In the carbide insertion testing, there is a noticeable decrease in k_{eff} as more uranium carbide fuel is added to the core. This along with the decrease in fast flux as a result of interactions with the fuel is given in Figure 6.16 and Figure 6.17. There is also a linear increase in fuel cost as a result of carbide insertion that is portrayed in Table 15. Note that the attempt to provide uniform insertion of carbide assemblies led to Design G having a greater k_{eff} value than the other cores; but this added value was offset by the decrease in peak fast flux that was observed.

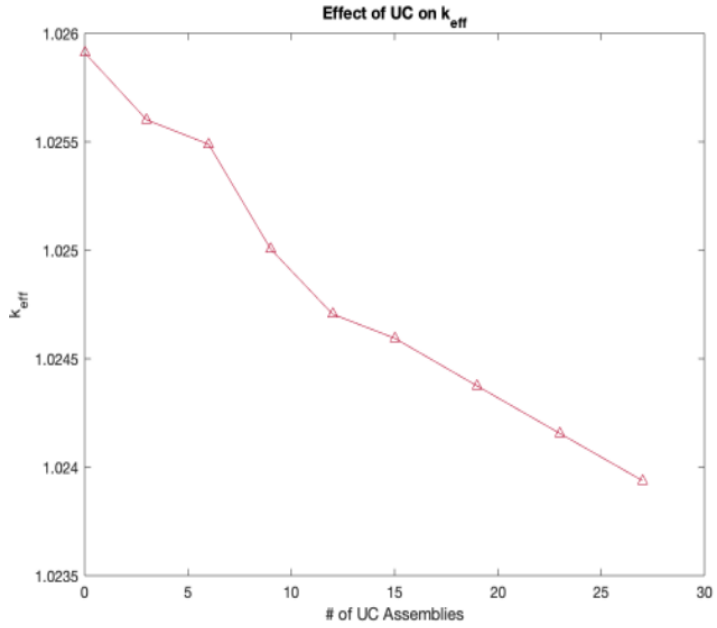

Figure 6.16: Carbide Effect on k_{eff}

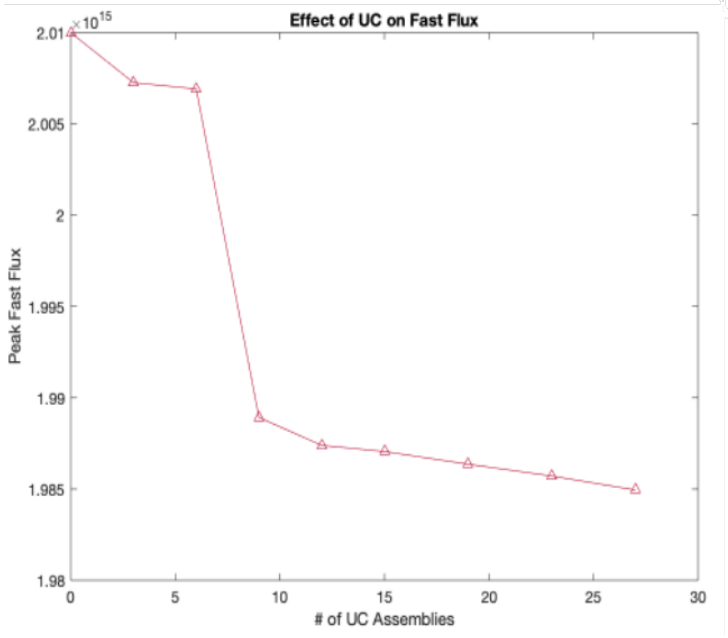

Figure 6.17: Carbide Effect on Fast Flux

Alongside the carbide insertion process was a metallic fuel insertion process which allowed for the effect of additional U-10Zr assemblies to be visualized. While the resulting fast flux and k_{eff} proved to be at values that were unfavorable by comparison to previous results, it did solidify the idea that metallic fuel provides the best functionality for the optimal core performance.

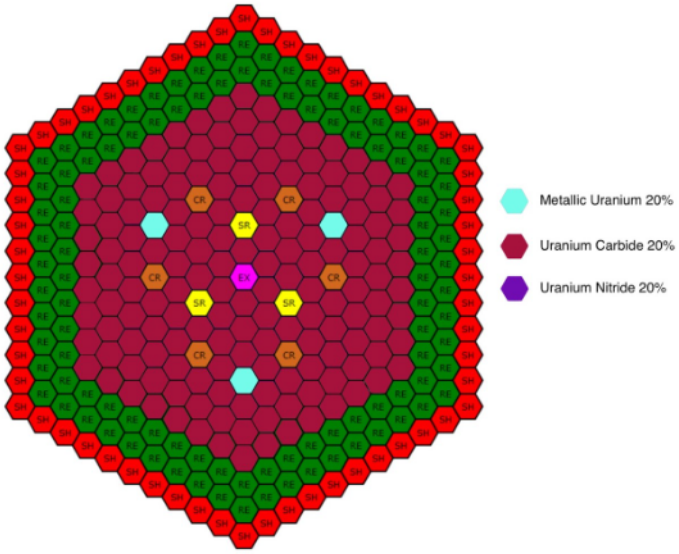

Figure 6.18: Metallic Insertion Design A

Design	Peak Fast Flux	k_{eff}	# of Metal FA	Front-End Cost
A	1.84E+15	1.01374	3	$278,659,000.00
B	1.84E+15	1.0138	6	$278,129,000.00
C	1.85E+15	1.01409	9	$277,599,000.00
D	1.85E+15	1.01427	12	$277,069,000.00
E	1.85E+15	1.01433	15	$276,538,000.00
F	1.85E+15	1.01446	19	$275,831,000.00
G	1.85E+15	1.01459	23	$275,124,000.00
H	1.86E+15	1.01472	27	$274,417,000.00

Table 16: Zirconium Insertion Test Results

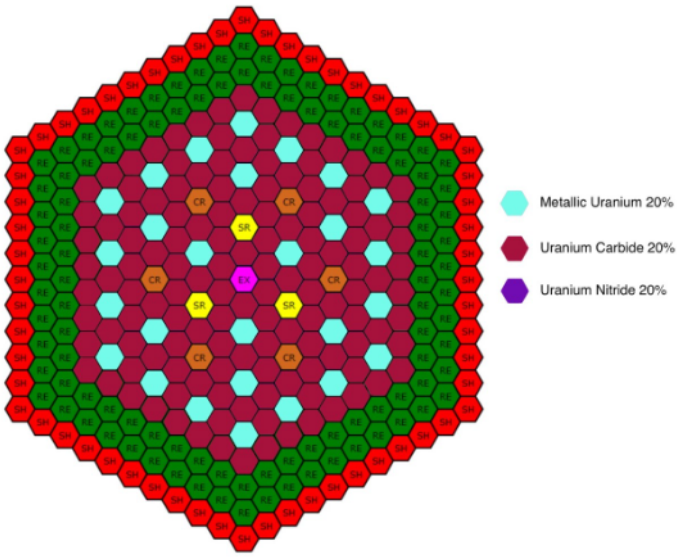

Figure 6.19: Metallic Insertion Design H

In observing the results of the metallic fuel insertion process, one of the relevant factors to include is the higher fuel costs at approximately $20 million more for metallic insertion than carbide insertion: meaning that the greatest benefit comes from preserving a metallic core and modifying it for slight differences in peak fast flux and k_{eff} values.

7 Depletion

The depletion results describe how the core characteristics change over time, most notably the core k_{eff}. The fission process continuously lowers the concentration of fuel isotopes, in our case U-235, and increases the concentration of fission products and poisons, isotopes which have a high neutron absorption cross section and thus remove neutrons from the reaction. Both of these processes serve as a source of negative reactivity, lowering the core k_{eff}.. It is, however, possible for a fast reactor to breed its own fuel. Fuel breeding occurs when a fertile isotope absorbs a neutron and undergoes a series of decays until it becomes a fissile isotope, which serves as a fuel in the chain reaction. The most notable example of fuel breeding occurs when U-238 absorbs a neutron, becoming U-239 before decaying into Pu-239, which is fissile. The conversion ratio is defined as the ratio of the production rate of fissile isotopes to the consumption rate of fissile isotopes, meaning that when the production ratio is unity, the number of fissile isotopes in the reactor is constant.

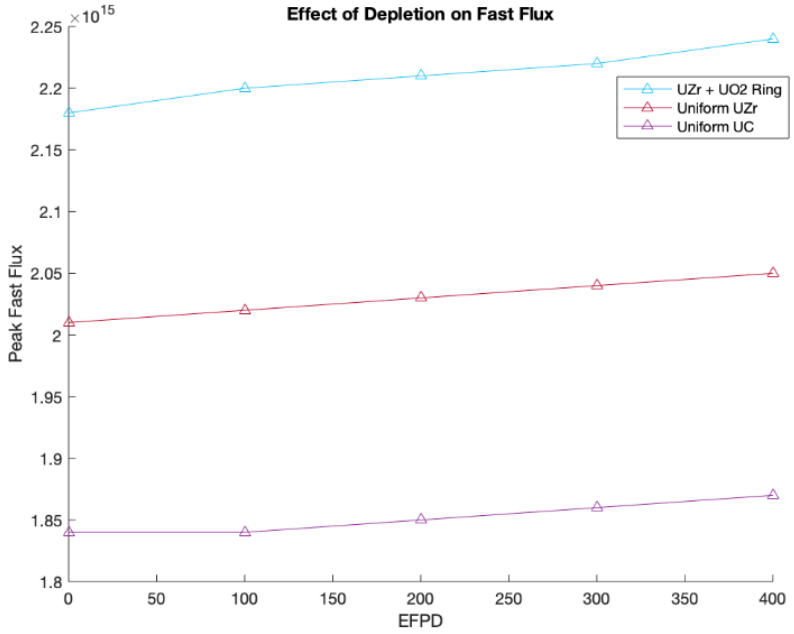

Figure 7.1: Depletion Effect on Fast Flux

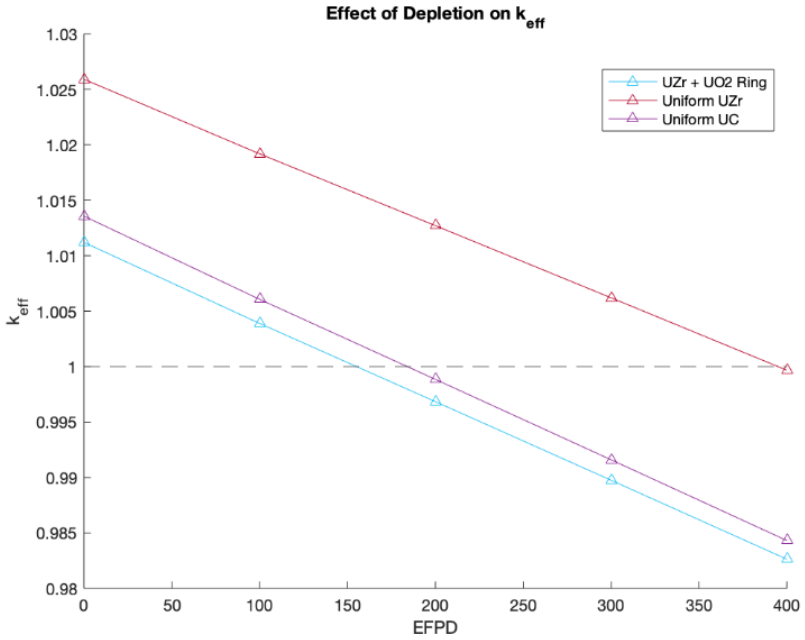

Figure 7.2: Depletion Effect on k_{eff}

Figure 7.1 and 7.2 portray the effect of depletion on peak fast neutron flux and k_{eff} for three different core designs. These were developed due to an interest in the performance each provided. While not listed as a priority due to the evaluation of fuel properties presented, the uranium oxide ring placed around the core led to a favorable k_{eff} value that is worth noting for future studies. In terms of fast flux generated following depletion, Figure 7.1 displays an increase over the effective full power days provided.

EFPD	k_{eff}
0	1.0112
100	1.00389
200	0.99684
300	0.98975
400	0.98263

Table 17: U-10Zr + UO2 Core Depletion

EFPD	k_{eff}
0	1.02590946
100	1.019184036
200	1.012707462
300	1.006200958
400	0.999672898

Table 18: Uniform U-10Zr Core Depletion

EFPD	k_{eff}
0	1.013569547
100	1.006063847
200	0.998846866
300	0.991593719
400	0.984314578

Table 19: Uniform UC Core Depletion

EFPD	k_{eff}
0	1.022296966
100	1.01542992
200	1.008821238
300	1.002181456
400	0.995518871

Table 20: Checkerboard-3 Core Depletion

The core underwent depletion under scenarios with Checkerboad-3, a uniform core of metallic fuel, a uniform core of carbide fuel, and an In-Out design with zirconium fuel and a single ring of oxide fuel. Following 100 EFPD increments, it was possible to determine the length of each fuel cycle. With this information gathered from depletion, it becomes possible to observe both the annual fuel cycle cost and the levelized cost of fuel (LCOF).

Design Type	EFPD	Peak Fast Flux	LCOF ($/MWh)	Annual Fuel Cost
Uniform U-10Zr	300	2.04E+15	$290.61	$248,359,475.10
Uniform UC	100	1.84E+15	$969.41	$828,481,769.28
U-10Zr + UO2	100	2.20E+15	$842.87	$720,338,295.12
Checkerboard-3	300	2.04E+15	$296.13	$253,080,419.10

8 Data Summary

Following multiple attempts to design a uranium core which could match the performance of plutonium fuel, it was found that the costs for reaching an equivalent fast flux value within the core would lead to the diminishing of characteristics which make the Versatile Test Reactor unique. While some facilities are capable of reaching a similar fast flux value, the VTR is also meant to function with various materials and coolant testing assemblies. Of the results gathered, the uniform U-10Zr core and the Checkerboard-3 design functioned as the best cases: providing 50% of the desired flux value for the core over an equivalent amount of EFPD to the original design. If the design limits were exceeded, such as a transition from HALEU to Highly-Enriched Uranium (HEU), it would likely reach the peak fast flux required while allowing for the core to maintain its initial functionality as a materials test reactor. Under such circumstances, the use of a uniform core of metallic fuel and the checkerboard design would require further investigation.

9 References

[1] Al-Dawood, K. (2021). Modeling, Simulation and Optimization of Lead-Cooled Fast Reactors (thesis).

[2] A. J. Brunett, and T. H. Fanning, U.S. Sodium Fast Reactor Codes and Methods: Current Capabilities and Path Forward, International Conference on Fast Reactors and Related Fuel Cycles, FR17, 26–29 June 2017 Yekaterinburg, Russian Federation

[3] Carlson, L., Wu, Z., Olson, J., and Liu, L. (E. (2020). An economic cost assessment on HALEU fuels for small modular reactors. Science and Technology of Nuclear Installations, 2020, 1–6. https://doi.org/10.1155/2020/8815715

[4] Cochran, R. G., and Tsoulfanidis, N. (1999). The Nuclear Fuel Cycle: Analysis and Management. American Nuclear Society.

[5] Crawford, D. C., Porter, D. L., and Hayes, S. L. (2007). Fuels for sodium-cooled fast reactors: US perspective. Journal of Nuclear Materials, 371(1-3), 202–231. https://doi.org/10.1016/j.jnucmat.2007.05.010

[6] D. Petti., et al., Advanced Demonstration and Test Reactor Options Study, INL/EXT-16-37867, Revision 2, July 2016.

[7] Ekberg, C., Ribeiro Costa, D., Hedberg, M., and Jolkkonen, M. (2018). Nitride fuel for Gen IV Nuclear Power Systems. Journal of Radioanalytical and Nuclear Chemistry, 318(3), 1713–1725. https://doi.org/10.1007/s10967-018-6316-0

[8] F. Heidet and R. N. Hill, Reactor Neutronics: Impact of Fissile Material, Nuclear Science and Engineering, 187:2,p. 202-211 (2017)

[9] Hassan, I. A., Badawi, A. A., El Saghir, A., and Shaat, M. K. (2019). Viability of uranium nitride (UN) as annular fuel for AP-1000. Progress in Nuclear Energy, 110, 170–177. https://doi.org/10.1016/j.pnucene.2018.09.020

[10] Hofman, G. L., and Walters, L. C. (2006). Metallic Fast Reactor Fuels. Materials Science and Technology. https://doi.org/10.1002/9783527603978.mst0105

[11] INL (Idaho National Laboratory), 2017, Advanced Demonstration and Test Reactor Options Study,INL/EXT-16-37867, Rev. 3, ART Program, Idaho Falls, Idaho, January.

[12] J. L. Rowlands, "Physics of fast reactor control rods", Progress in Nuclear Energy, vol. 16, no 3, pp 287-321, 1985

[13] Judkins, R., and Olsen, A. (1979). Nuclear fuel fabrication and refabrication cost estimation methodology. https://doi.org/10.2172/5819027

[14] Matthews, R. B., Chidester, K. M., Hoth, C. W., Mason, R. E., and Petty, R. L. (1988). Fabrication and testing of uranium nitride fuel for space power reactors. Journal of Nuclear Materials, 151(3), 345. https://doi.org/10.1016/0022-3115(88)90029-3

[15] M. D. Carelli and A. J. Friedland, "Hot channel factors for rod temperature calculations in LMFBR assemblies",Nuclear Engineering and Design 62 (1980) 155-180

[16] Murty, K. L., and Charit, I. (2013). An Introduction to Nuclear Materials: Fundamentals and Applications. Wiley-VCH.

[17] NEPA Policy and Compliance, Draft Versatile Test Reactor Environmental Impact Statement (2020). DOE

[18] NRC (U.S. Nuclear Regulatory Commission), 1994, Preapplication Safety Evaluation Report for the Power Reactor Innovative Small Module (PRISM) Liquid-Metal Reactor, NUREG-1368, Washington, DC, February.

[19] Palmtag, S. (2019). Lecture notes on NE301. North Carolina State University.

[20] Palmtag, S. (2021). Lecture notes on LUPINE. North Carolina State University.

[21] Hou, J. (2021). Lecture notes of NE412/NE512 Nuclear Fuel Cycle. North Carolina State University.

[22] UxC (2021). UxC Nuclear Fuel Price Indicators.

[23] Vasudevamurthy, G., and Nelson, A. T. (2021). Uranium carbide properties for Advanced Fuel Modeling – A Review. Journal of Nuclear Materials, 153145. https://doi.org/10.1016/j.jnucmat.2021.153145

[24] Youinou, G., Bays, S., Palmiotti, G., Heidet, F., Fei, T., Smith, M. (2020). Scoping analysis of sodium cooled fast spectrum test reactor cores. https://doi.org/10.2172/1598332